

HYDRAULICS OF LOW GRADIENT  
BORDER IRRIGATION SYSTEMS

by

Norman A. Evans, Dale F. Heermann,  
Orlando W. Howe, Dennis C. Kincaid

June 30, 1970

COLORADO WATER RESOURCES



RESEARCH INSTITUTE

**Colorado State University**  
**Fort Collins, Colorado**

Completion Report Series No. 19

HYDRAULICS OF LOW-GRADIENT BORDER  
IRRIGATION SYSTEMS

Completion Report

OWRR Project B-024-COLO

June 30, 1970

by

Norman A. Evans  
Dale F. Heermann  
Orlando W. Howe  
Dennis C. Kincaid

Department of Agricultural Engineering  
Colorado State University

submitted to

Office of Water Resources Research  
U. S. Department of Interior  
Washington, D. C.

The work upon which this report is based was supported (in part) by funds provided by the United States Department of the Interior, Office of Water Resources Research, as authorized by the Water Resources Research Act of 1964, and pursuant to Grant Agreement No. 14-01-001-1883

Colorado Water Resources Research Institute  
Colorado State University  
Fort Collins, Colorado

Norman A. Evans, Director

## ABSTRACT

### HYDRAULICS OF LOW-GRADIENT BORDER IRRIGATION SYSTEMS

Surface flow data from field experiments on 21 borders were analyzed to determine parameters characterizing infiltration and surface retardance. Infiltration constants for a logarithmic intake function were determined by the use of cylinder infiltrometers and by using the entire border as an infiltrometer. The borders were constructed on a clay loam soil which exhibited cracking when dry. The infiltration analysis showed that for this type of soil, the cylinder infiltrometers underestimate the infiltrated depth by nearly 50 percent.

Resistance parameters were calculated by a volume balance procedure after the intake constants were determined.

A mathematical model simulating border irrigation was developed by using the theory of unsteady hydrodynamics. The momentum and continuity equations were solved numerically by the method of characteristics. The advance of the wetting front was controlled by the requirement that the sum of the surface storage and infiltrated volumes must equal the total volume applied at all times.

Dimensionless curves were derived relating the average surface storage depth to the advance distance. These curves allow a simple volume balance procedure to be used for predicting advance with constant inflow rates.

Further work needs to be done to extend the hydrodynamic theory to the recession phase and to apply the results to a national design procedure for border irrigation systems.

## I. Introduction

Surface irrigation methods are used to apply water on more than 60% of all lands irrigated, yet efficiency of water utilization under current practices is seriously low. Substantial savings in water can be realized if better design and operating criteria are developed and made available to the engineering profession.

Efficiency of surface irrigation methods has been given limited technical attention. Willardson and Bishop (18) presented a method of estimating border irrigation efficiencies as influenced by the soil intake rate, time for water to reach the end of the border and time for a desired depth of water to infiltrate into the soil. Shockley, Woodward and Phelan (16) presented a quasi-rational method of border irrigation design based on the requirement of a given irrigation depth. They emphasized that the most uniform irrigation could be obtained if the intake opportunity time were the same for the entire length of border.

One of the earliest references to the concept of uniform intake opportunity time was that of Lewis and Milne (12). They pointed out that equal advance and recession time provides uniform intake opportunity time and may be obtained approximately by stopping inflow at the proper time before the advancing front reaches the end of the border.

### Maximum Irrigation Efficiency

Even though the concept of maximum efficiency resulting

from uniform intake opportunity times has been recognized, this idea has received little research attention. Irrigation systems have been generally designed to require the fewest possible number of irrigations per season. For this to be accomplished, the maximum allowable soil water deficit must be reached in the root zone prior to each irrigation and then the water storage capacity of the root zone must be completely refilled. Advantages of this design are that fewer irrigations result in less water loss by evaporation during and immediately following irrigation and labor requirements are minimal. However, this approach has proved to be inadequate for water conservation because available root zone storage is not equal for all crops in a rotation, and will change during the season for most crops. A border designed for a high application depth cannot be given a small application efficiently when this is desired.

One alternative is a system design which does not aim to achieve a given depth of application, but which strives to achieve maximum possible efficiency. This requires accepting the resulting application depth and meeting water demand requirements by irrigating with the necessary frequency. This approach has become practicable as modern water supplies become available on demand and new developments in automation of irrigation operations (3) eliminating much of the labor requirement. Without these conditions, of course, such an approach would not be possible.

### Historical Background

Development of a rational design procedure was the goal laid out for an extensive and long term irrigation research program in Colorado beginning in 1955. The program was jointly planned and

conducted by the USDA Agricultural Research Service and the Colorado State University Experiment Station.<sup>1/</sup> Experiment Station support was approved through a Western Regional Research Project (W-65) administered by the Cooperative State Research Service.

Initial studies sought to find a technique for describing surface roughness with which direct prediction of hydraulic resistance could be made. Laboratory flume studies using natural soils fixed in place and steady, uniform flows were reported by Kruse et al. (11). Evans and Heermann designed field experiments<sup>2/</sup> to test the laboratory findings under nonuniform flow and normal soil conditions. Findings were reported by Heermann (5) in a masters thesis and extended by Wenstrom (17) in another masters thesis. These experiments clearly indicated that surface roughness on irrigated soil could be characterized by the standard deviation of roughness element heights,  $\sigma$ . Direct measurement of the parameter,  $\sigma$ , provides sufficient information with which to estimate hydraulic resistance.

Examining the possibility that an additional parameter describing roughness element spacing might improve the estimate of hydraulic resistance, Heermann (6) used sinusoidal roughness elements in a pipe with air for the fluid. The result of these experiments was that no spacing function could be found to improve upon  $\sigma$  alone. Upon further study he discovered that  $\sigma$  automatically accounts for element density, a fact which he verified using

---

<sup>1/</sup> USDA project leader was August R. Robinson; CSU project leader was Norman A. Evans.

<sup>2/</sup> Colorado participating project in Western Regional Research Project W-65.

published hydraulic resistance data of Schlicting (15), Koloseus et al. (9), and Sayre et. al. (14).

With the technique for hydraulic resistance estimation established, attention was next turned to the infiltration characteristic of an irrigated soil. Simultaneously, field experiments were initiated to establish operating criteria for maximum irrigation efficiency in border irrigation systems. These experiments have been reported in the Completion Report covering OWRR Project B-001-COLO. This report is essentially a phase II or extension of that project.

### Objectives

The objectives of this study were as follows:

1. Determine coefficients for empirical intake functions utilizing the entire border as an infiltrometer and compare these with coefficients determined from cylinder infiltrometers.
2. Determine the resistance to flow under different cropping conditions.
3. Integrate the empirical intake and resistance parameters into a rational design procedure for low gradient irrigation borders.

The theory and results of the infiltration analysis under objective 1 are given in Part II of this report. Methods of analysis for determining resistance to flow have been developed under objective 2 and the resistance parameter has been computed from data collected during a large number of irrigations.

In regard to the last objective, a mathematical model simulating border irrigation flows has been developed which utilizes

the calculated parameters (8). The theory is summarized in Part III of this report. The model can be used for predicting the rate of water advance in border systems for specified resistance and infiltration. Knowledge of advance and recession functions is required in any rational irrigation system design procedure.

## II. Infiltration Analysis

### Field Experiments

Infiltration constants and resistance parameters were evaluated from experimental data on field borders. Data were collected at two sites near Grand Junction, Colorado. At Site S, there were 8 borders approximately 1100 feet long and 30 feet wide. These borders has slopes of 0.004 to 0.005 feet per foot. Site M had 13 borders approximately 25 feet in width with lengths of from 650 to 800 feet. The slopes at Site M ranged from 0 to 0.001 feet per foot.

The Grand Junction borders were constructed on clay loam soils having relatively low intake rates. Crops were brome-grass, alfalfa, and milo. Physical dimensions and further descriptions of the experimental borders are given by Howe and Heermann (7).

### Procedure

Gilley (1) described in detail the experimental procedures and methods of analysis for obtaining infiltration constants. These will be summarized briefly, after which the determination of resistance parameters will be discussed.

On each border, steel bench marks for measuring water surface elevations were located at every 100 foot station except zero. At Site M, additional bench marks were located at 25, 50, 75, and 150 feet. During each irrigation, advance and recession data were collected consisting of the time of arrival at each bench mark location of the advancing or receding edge. After

arrival at a bench mark station, the depth of water was measured every few minutes for a sufficient number of times to describe the hydrograph as a series of straight lines. Hydrographs for station zero were estimated.

Cross-sectional topographic data were taken at 10 foot intervals on each border to determine the average slope and to facilitate calculation of average flow depths. By constructing water surface profiles from hydrograph data the surface storage and infiltrated volumes were determined at specified intervals of time.

#### Infiltration Function and Border Infiltrometer

The desirable characteristics of an infiltration function for border irrigation are simplicity and agreement with field infiltration observations under flooding conditions. A function which describes the infiltration rates of many soils is the Kostiakov equation (10)

$$I = k\tau^{(a-1)} \quad , - - - (1)$$

where I is the infiltration rate

$\tau$  is the intake opportunity time

and k and a are constants.

Gilley (1) developed a procedure for determining the constants in Equation 1 using experimental field data on advance and surface storage volume. Integration of Equation 1 gives

$$z = K\tau^a \quad , - - - (2)$$

where z is the infiltrated depth

K is the constant  $k/a$

a is the exponent

and  $\tau$  is the intake opportunity time.

The advancing front of water in a border strip is described reasonably well by the function,

$$s = b t^h \quad , \quad - \quad - \quad - \quad (3)$$

where  $s$  is the advance distance

$t$  is the time that water has been on the border

and  $b$  and  $h$  are empirical constants.

At any given distance  $x$  the intake opportunity time is the difference between the advance time to  $x$  and the total elapsed time. This difference is

$$\tau_x = (s/b)^{1/h} - (x/b)^{1/h} \quad , \quad - \quad - \quad - \quad (4)$$

The time interval defined in Equation 4 is substituted into Equation 2, giving the infiltrated depth at the distance  $x$ . The depth is then integrated with respect to distance to obtain the infiltrated volume by the equation

$$V_z = B \int_0^s K \left[ (s/b)^{1/h} - (x/b)^{1/h} \right]^a dx \quad , \quad - \quad - \quad - \quad (5)$$

where  $V_z$  is the total infiltrated volume,

and  $B$  is the border width.

Changing the variable of integration from  $x$  to  $t$ ,

$$V_z = B \int_0^{t_s} K b h (t_s - t)^a t^{h-1} dt \quad , \quad - \quad - \quad - \quad (6)$$

Equation 6 can be integrated term by term after expanding the expression  $(t_s - t)^a$  in a binomial series. After performing the integration

$$V_z = B K b h t_s^{a+h} f(a, h) \quad , \quad - \quad - \quad - \quad (7)$$

where  $f(a, h) = \frac{1}{h} - \frac{a}{h+1} + \frac{a(a-1)}{2!(h+2)} - \frac{a(a-1)(a-2)}{3!(h+3)} + \dots$  - (8)

The values of  $b$ ,  $h$ ,  $K$  and  $a$  are assumed constant for each

irrigation. The advance constants  $b$  and  $h$  are determined from the advance data. The infiltrated volume defined by Equation 7 is a logarithmic function of  $t$ . Therefore, a plot of  $V_z$  versus  $t$  on log-log paper should be a straight line with slope  $a+h$ . With  $a+h$  known, the constant can be found and the function  $f(a,h)$  can be calculated. Substituting the infiltrated volume at  $t = 1$  and the constants  $B, b, h$  and  $f(a,h)$  into Equation 7, the constant  $K$  is determined.

#### Comparison of Cylinder and Border Infiltrometer Constants

Cylinder infiltrometers are frequently used to characterize the intake function of a particular soil. Haise, et al. (2) published a bulletin describing the use of cylinder infiltrometers for determining intake characteristics of irrigated soil. In the standardized procedure, the intake cylinder is filled with water to a depth of 4 to 5 inches. Immediately after filling, a hook-gauge measurement of the water surface elevation is recorded and assumed to be the depth at the starting time. This technique of determining the initial depth is questionable, especially on soils with high initial intake rates.

The cylinder infiltrometer procedures were modified for this study by adding a known volume of water to the infiltrometer and calculating a depth at the starting time. With the known initial depth, the data were analyzed by fitting the logarithmic intake function to the accumulated depth versus time data.

An analysis was also made of the cylinder infiltrometer data assuming that the initial depth was an unknown. This analysis curve fit the infiltration rate versus time function. The

rate was determined from the depth infiltrated between consecutive readings and plotted at the mid-point of time.

The infiltration functions determined by using the border as an infiltrometer are assumed to be the most accurate. Table 1 presents data comparing the infiltrated depth determined from the border infiltration constants and the average depth applied. The average infiltrated depth was calculated using the infiltration function and the observed average intake opportunity times for the given irrigation. The applied depth for each irrigation exceeds the depth estimated by the infiltration function. This difference can be accounted for in the volume of water which remained on the surface at the time recession was observed. The water was assumed to have receded when the water surface reached the level of the bench marks on the edge of the border. These bench marks were set at an elevation equal to the average of the crest elevations across the border. The water contained in the corrugations below the crests is approximately equal to one surface inch. Longitudinally, the borders were not established to a uniform grade which also account for differences between the applied depth and average infiltrated depth. Examination of the data by individual borders and individual years indicates that the differences are the same for a given border on a given year. On the basis of this information, it is assumed that the border infiltrometer accurately estimates the infiltrated depth and is a basis for comparing the cylinder infiltrometer data. The depth infiltrated in a 90-minute period was calculated with the infiltration constants determined by the border method and by the cylinder accumulated depth method. These depths are compared in

Figure 1. The border method for determining the infiltration constants generally indicates a larger infiltrated depth than does the cylinder accumulated depth method. The ratio of infiltrated depth from the cylinder depth method to the infiltrated depth by the border method is equal to 0.58 with a standard error of 0.035. The cylinder rate method estimates an even smaller infiltrated depth as shown in Figure 2. The ratio of infiltrated depths from the cylinder rate and border methods is 0.43 with a standard error of 0.025. This data leads to the conclusion that on a clay loam soil which exhibits considerable cracking, it would be necessary to increase the infiltrated depth determined by cylinder constants when applying cylinder data to field conditions.

The infiltration functions are primarily used in estimating the advance of a border stream. Figure 3 compares the measured empirical advance distances with advance distances calculated by the Phillip and Farrell solution (13) utilizing the infiltration constants and an observed average surface storage depth. The various symbols represent the infiltration functions determined from the border, cylinder accumulated depth, and cylinder rate method. Table 2 presents the mean percent differences between the empirical and corresponding calculated advance distances for the various infiltration constants. The 20 and 30 percent differences occurring when utilizing the cylinder infiltration constants emphasizes the need for an accurate determination of the true infiltration function. The functions determined using the border method have only a 2 percent mean error for Site S and the milo on Site M compared to a 10 percent mean error with the alfalfa on Site M.

TABLE 1

COMPARISON OF AVERAGE APPLIED IRRIGATION DEPTH AND INFILTRATED DEPTH DETERMINED FROM BORDER INFILTRATION CONSTANTS AND OBSERVED INTAKE OPPORTUNITY TIME FOR SITE S.

Border	Year	(1)	(2)	Difference 1 - 2 inches
		Average Applied Depth inches	Average Infiltrated Depth inches	
2	1966	3.8	3.7	0.1
4	1965	3.3	2.2	1.1
4	1966	4.9	4.1	0.8
5	1965	2.7	1.6	1.1
5	1966	4.6	4.1	0.5
5	1966	4.3	3.8	0.5
6	1965	3.3	2.5	0.8
6	1966	4.4	3.4	1.0
6	1966	3.6	2.5	1.1
7	1966	4.7	4.1	0.6
8	1965	3.2	3.1	0.1
8	1966	3.4	3.2	0.2

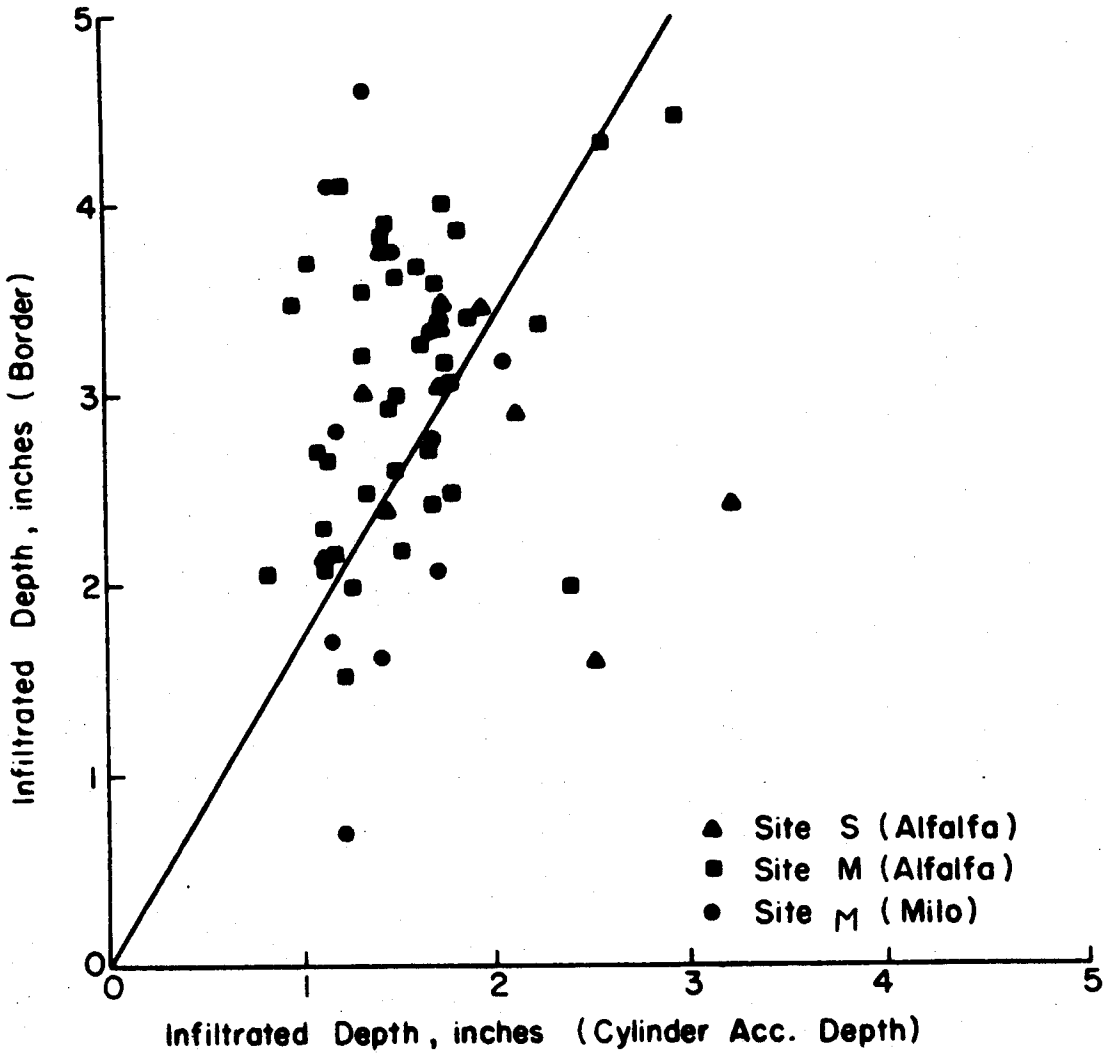


Figure 1. Comparison of infiltrated depths calculated with infiltration constants determined by border and cylinder accumulated depth method. (Depths at 90 minutes)

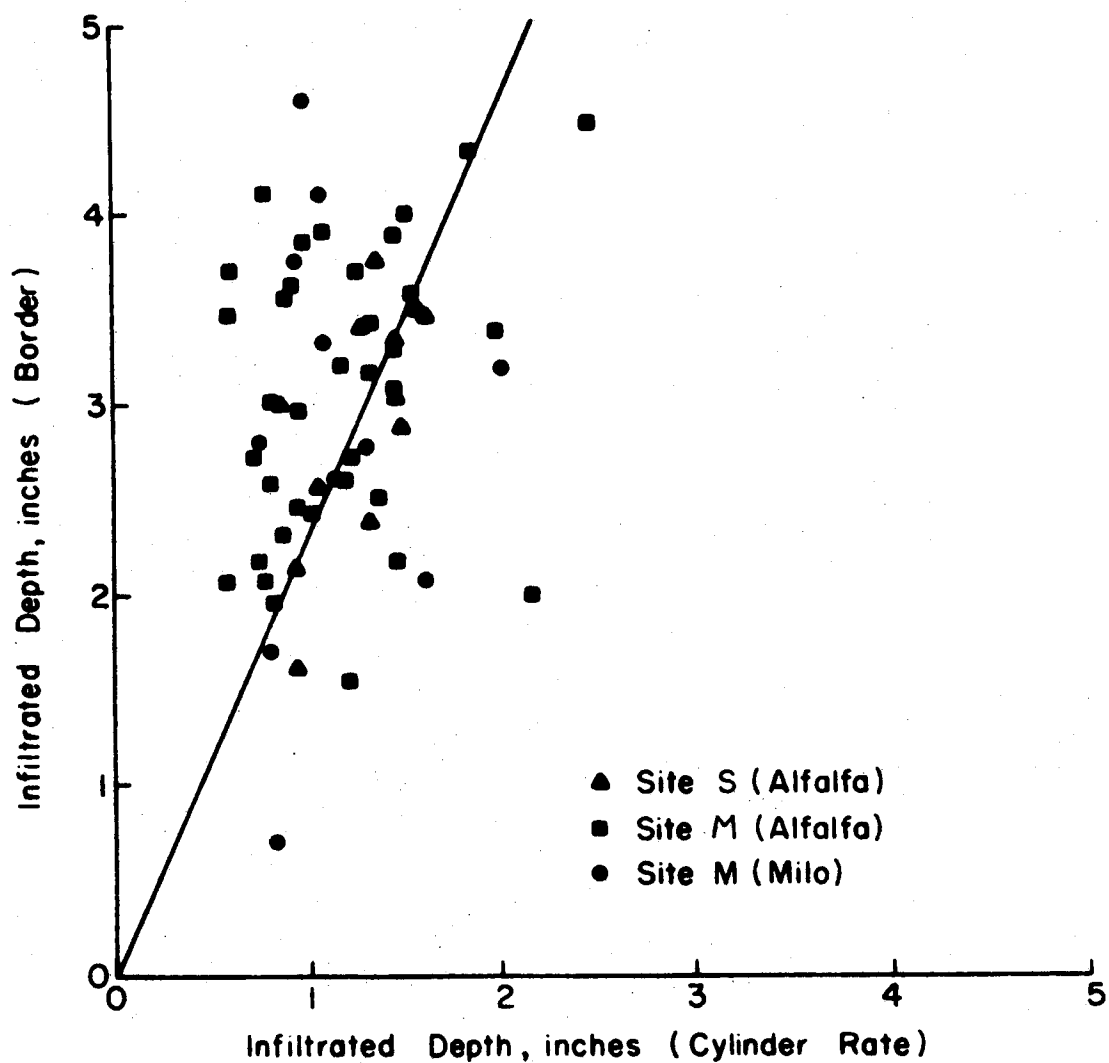


Figure 2. Comparison of infiltrated depths calculated with infiltration constants determined by border and cylinder rate methods (Depths at 90 minutes)

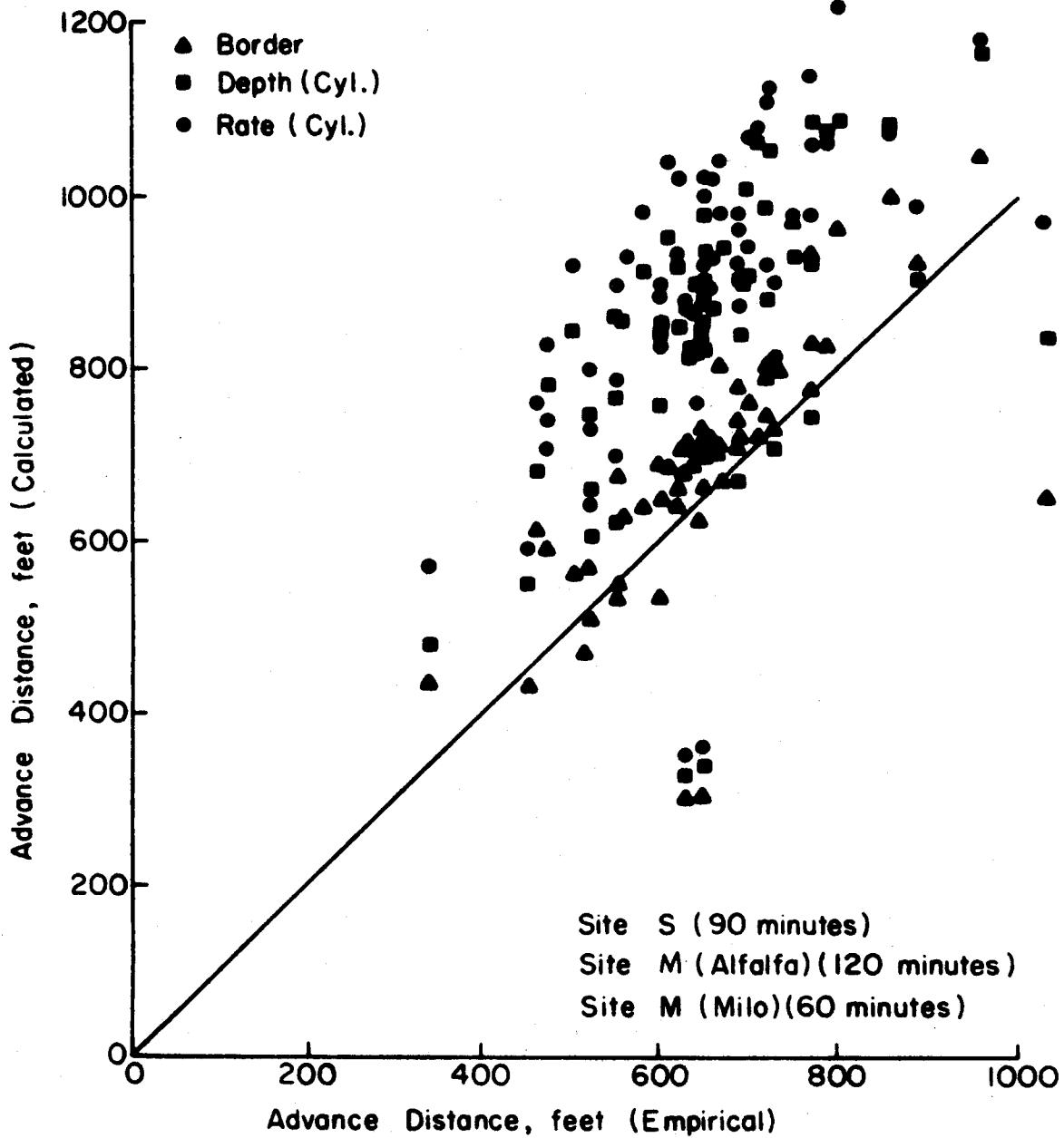


Figure 3. Comparison of advance distances calculated from infiltration constants vs the measured empirical distances.

TABLE 2

MEAN PERCENT DIFFERENCE BETWEEN  $s = bt^h$  AND THE ESTIMATION OF ADVANCE RATE WITH INFILTRATION FUNCTIONS USING PHILLIP AND FARRELL TECHNIQUE.

	Site S	Site M	
	Alfalfa - Bromegrass %	Alfalfa %	Milo %
Empirical - Border	2	10	2
Empirical - Cyl. Depth	21	25	23
Empirical - Cyl. Rate	34	44	34

Volume Balance Calculation

Once the infiltration constants have been determined, the following procedure can be used to calculate flow rates at downstream sections as illustrated in Figure 4. The flow rate through any downstream cross-section is equal to the inflow at the upper boundary minus the outflow due to infiltration and increasing surface storage upstream of that section.

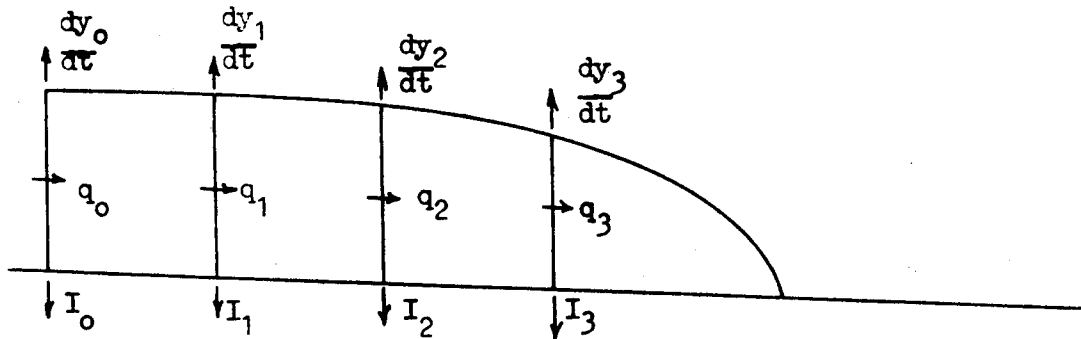


Figure 4. Calculation of Downstream Flow Rates

If the inflow  $q_{i-1}$  to any channel reach of length  $\Delta x$  is known, the outflow from that reach is

$$q_i = q_{i-1} - \frac{\Delta x}{2}(I_i + I_{i-1} + \frac{dy_i}{dt} + \frac{dy_{i-1}}{dt}) , \dots (9)$$

where  $q_i$  is the flow rate per unit width leaving the  $i$ th reach

$I_i$  is the infiltration rate at  $x = i\Delta x$

and  $\frac{dy_i}{dt}$  is the rate of rise of the water surface at  $x = i\Delta x$ .

The rate of rise of the water surface at a hydrograph station is defined as the slope of the hydrograph at the particular instant. The depth and rate of rise at points between hydrograph stations are determined by linear interpolation from the two nearest hydrographs. The infiltration rates are determined by intake opportunity time which is the total elapsed time minus the arrival time to a particular point on the border. The arrival time is

determined by logarithmic interpolation between the arrival times for the two nearest hydrographs.

The flow rates are calculated for stations 10 feet apart starting at the upper boundary and ending at a point about 30 feet behind the advancing front. Average velocities are defined by the relation  $V_i = q_i/y_i$ , where  $y_i$  is the average depth determined from the water surface elevation and mean border elevation at any 10 foot station. The total head at each station is calculated by adding the velocity head to the water surface elevation at that point. The slope of a straight line fitted by least squares regression through the total head data defines the average energy gradient. Energy gradients are calculated for the entire reach and for each 100 foot increment. Resistance parameters are calculated by substituting the energy gradient, average depth and average velocity for a given length of channel into a resistance function of the following type.

It is assumed that the energy gradient in gradually varied flow is equal to the slope of a uniform flow of the same depth and velocity. Two equations which have historically been used to describe uniform flow are the Chezy equation,

$$V = C\sqrt{RS_0} \quad , \quad - \quad - \quad - \quad (10)$$

and the Manning equation

$$V = \frac{1.49}{n} R^{2/3} S_0^{1/2} \quad , \quad - \quad - \quad - \quad (11)$$

where  $V$  is the mean velocity

$S_0$  is the channel bottom slope

$R$  is the hydraulic radius

and  $C$  and  $n$  are resistance coefficients.

In border flow the hydraulic radius may be replaced by the

average depth. Substituting the energy gradient for the bottom slope and rearranging, the above equations take the form

$$C_f = S_f \frac{Y^p}{V^2} \quad , \quad - \quad - \quad - \quad (12)$$

where  $C_f$  is a general resistance coefficient

$S_f$  is the energy gradient

and  $p$  is a constant ( $p = 1$  for the Chezy equation and  $p = 4/3$  for the Manning equation).

### III. A Hydrodynamic Model of Border Irrigation

Border irrigation is characterized by shallow flow on a plane sloping bed with uniform surface retardance and infiltration properties. Since the depths are small relative to the width of the border, the flow is analyzed on a unit width of channel.

The equations governing unsteady, spatially varied flow in a wide channel are the continuity equation,

$$y \frac{\partial V}{\partial x} + V \frac{\partial y}{\partial x} + \frac{\partial y}{\partial t} = -I \quad , \quad - \quad - \quad - \quad (13)$$

and the momentum equation,

$$\frac{\partial y}{\partial x} + \frac{V}{g} \frac{\partial V}{\partial x} + \frac{1}{g} \frac{\partial V}{\partial t} = \frac{IV}{gy} + S_o - S_f \quad , \quad - \quad - \quad - \quad (14)$$

where  $y$  is the flow depth - ft.

$V$  is the mean velocity - ft./sec.

$x$  is the distance from the upper end of the channel - ft.

$t$  is time from the beginning of inflow - sec.

$I$  is the infiltration rate - ft./sec.

$S_o$  is the border slope - ft./sec.

$S_f$  is the energy gradient - ft./ft.

and  $g$  is the acceleration of gravity - ft./sec.<sup>2</sup>.

A technique known as the method of characteristics is used to solve the differential equations. This method is described briefly here.

The above equations constitute a pair of quasi-linear, first order partial differential equations with independent variables  $x$  and  $t$ , and dependent variables  $y$  and  $V$ . This system of equations is of the hyperbolic type which have, at every

point of the x-t plane, two directions in which the integration of the partial differential equations reduces to the integration of equations involving total differentials only. For the given system these directions are specified by the equations

$$\left. \frac{dx}{dt} \right|_+ = V + \sqrt{gy} \quad , \quad - - - (15)$$

and  $\left. \frac{dx}{dt} \right|_- = V - \sqrt{gy} \quad , \quad - - - (16)$

These are called characteristic directions with Equation 15 specifying a forward characteristic and Equation 16 specifying a backward characteristic. It can be shown that along the characteristic lines described by the above relationships, the following ordinary differential equations are valid. Along a forward characteristic the depth and velocity are determined by the equation

$$\frac{d}{dt} (V + 2\sqrt{gy}) = g(S_o - S_f) + \frac{I}{y} (V - \sqrt{gy}) \quad . \quad - - - (17)$$

On a backward characteristic the values of V and y are determined by

$$\frac{d}{dt} (V - 2\sqrt{gy}) = g(S_o - S_f) + \frac{I}{y} (V + \sqrt{gy}) \quad . \quad - - - (18)$$

The method of characteristics involves locating the characteristic lines and then integrating Equations 17 and 18 along these lines.

The characteristic network for an advancing front on a plane bed with constant inflow at the upper boundary is shown in Figure 5. The wetting front constitutes a moving boundary at zero depth, where both the forward and backward characteristics have the same positive slope. Critical depth is located a short distance behind the wetting front and upstream from this point the flow is entirely

subcritical. The characteristic lines become straighter as normal depth is approached.

### Finite Difference Techniques

The characteristic network forms an irregular grid in the time-distance plane. It is possible to use a computational scheme which follows this network and calculates depths and velocities at irregularly spaced points. However, in this analysis it is advantageous to use a rectangular grid system and advance the solution over constant time intervals. Figure 6 illustrates the solution for one grid point and clarifies the notation. With the depth and velocity known at Points A, B, and C at time  $t$ , the unknown Point H can be solved in the following manner. The characteristic curves joining Point H to Points G and M are approximated by straight lines whose slopes are specified by the depth and velocity at Points G and M. Thus, Equations 15 and 16 can be approximated by

$$\frac{x_H - x_G}{t_H - t_G} = v_G + \sqrt{gy_G} \quad , \quad \text{--- (19)}$$

and 
$$\frac{x_H - x_M}{t_H - t_M} = v_M - \sqrt{gy_M} \quad . \quad \text{--- (20)}$$

Points G and M are allowed to move in the  $x$  direction so that the characteristics extended from them will intersect at the fixed Point H. The velocity and depth at Points G and M are determined by linear interpolation between Points A-B and B-C respectively.

In finite difference form Equations 17 and 18 become respectively after integrating

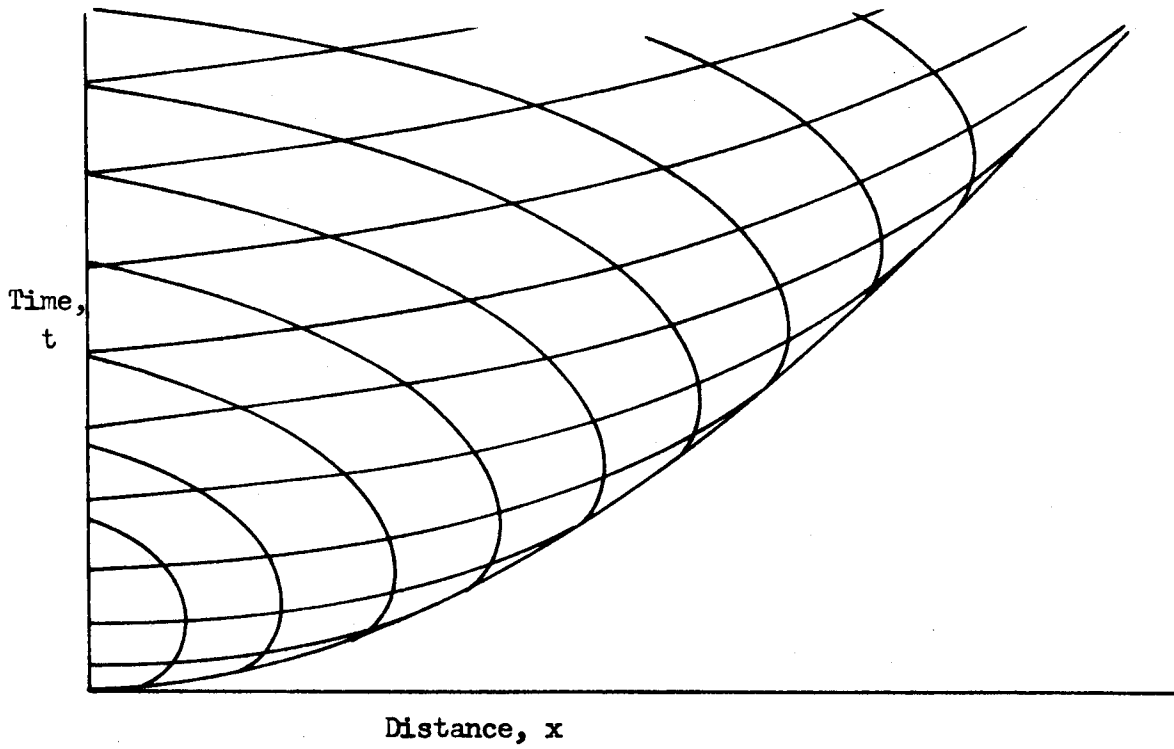


Figure 5. Characteristic Network for an Advancing Front

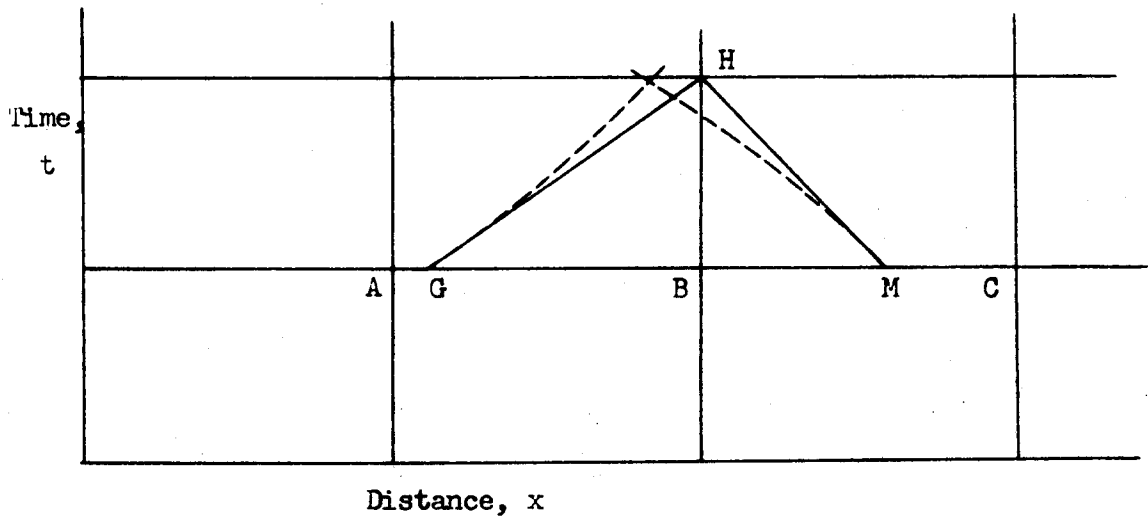


Figure 6. Method of Specified Time Intervals

$$V_H + 2\sqrt{gY_H} = V_G + 2\sqrt{gY_G} + \int_{t_G}^{t_H} \left[ g(S_o - S_f) + \frac{I}{Y}(V - \sqrt{gY}) \right] dt \quad , \quad (21)$$

and

$$V_H - 2\sqrt{gY_H} = V_M - 2\sqrt{gY_M} + \int_{t_M}^{t_H} \left[ g(S_o - S_f) + \frac{I}{Y}(V - \sqrt{gY}) \right] dt \quad . \quad (22)$$

The integrals are evaluated numerically by the trapezoidal rule. The value of the integral is equal to the time interval  $\Delta t$  multiplied by the average value of the integrand evaluated at the end points.

In solving the above equations the first step is to locate the characteristic lines and Points G and M by a simultaneous solution of the slope equations and interpolation formulas. With the depths and velocities at Points G and M known, the integration formulas are solved simultaneously for  $V_H$  and  $Y_H$ . The infiltration rates are evaluated by Equation 1 with  $k$  and  $a$  constant, and energy gradients are calculated by means of Equation 12, rearranged with the parameters  $C_f$  and  $p$  held constant.

This method allows for direct computation of interior points. With the time interval specified, the grid spacing in the  $x$  direction is made large enough so that Points G and M fall between the grid points from which they are interpolated. Grid points on the upper boundary are solved by using Equations 20 and 22 for the backward characteristic plus the boundary condition

$$q = v_U Y_U \quad , \quad - - - \quad (23)$$

where  $q$  is the unit inflow discharge

and  $U$  denotes a point on the upstream boundary.

The above method is called the initial slope method since the characteristic lines have slopes specified at the initial

points for each time increment. This approximation is inaccurate where the depth is changing rapidly with distance, as near the advancing front. A much better estimate of the slope of a line connecting two points on the same characteristic is obtained by taking the average of the characteristic slopes at the end points. However, the solution of interior points using average slopes is considerably more difficult than the initial slope method and requires a complicated iteration process. A compromise method is arrived at in the following manner.

In the type of flow under consideration the velocities are small and the curvature in the characteristics is mostly a result of the rapid change in depth with distance behind the wetting front. Hence, the unknown velocity  $V_H$  is not needed to accurately describe the slopes and Equations 15 and 16 can be written

$$\frac{x_H - x_G}{t_H - t_G} = V_G + \frac{1}{2} (\sqrt{gy_G} + \sqrt{gy_H}) \quad , \quad - \quad - \quad - \quad (24)$$

and

$$\frac{x_H - x_M}{t_H - t_M} = V_M - \frac{1}{2} (\sqrt{gy_M} + \sqrt{gy_H}) \quad , \quad - \quad - \quad - \quad (25)$$

These last two equations are used in the solution of interior points near the advancing front, along with Equations 21 and 22 to carry out the integrations. An iteration procedure is used to solve these equations simultaneously for  $V_H$  and  $y_H$ .

#### Advancing the Wetting Front

This section deals with the problem of determining the rate of advance of the wetting front with time. The problem of initiating a solution will be discussed later.

As stated previously, the wetting front is a moving boundary

advancing at some positive rate and a depth of zero. However, since the integration equations are undefined for  $y = 0$ , the computations must be started from an arbitrary positive depth. There are no usable boundary conditions for the advancing front.

If the moving boundary is located at critical depth the front may be assumed to be a vertical wall of water and the depth and velocity are related by the equation

$$V_T = \sqrt{gy_T} \quad , \quad - \quad - \quad - \quad (26)$$

where T denotes a point on the moving boundary. The local velocity  $V_T$  is equal to the rate of advance of the boundary itself.

In low gradient border flow the critical depths are very small. As critical depth is approached, the assumptions used in deriving the original differential equations are less valid and use of the Manning or Chezy equation to calculate energy gradients is questionable under these conditions. Therefore, in this analysis the moving boundary is located at some depth, considerably greater than critical depth, yet small relative to the upstream depths. The moving boundary is located behind the wetting front.

The rate of advance of the moving boundary is assumed constant for each time increment, and is given by

$$w = \frac{s_N - s_{N-1}}{\Delta t} \quad , \quad - \quad - \quad - \quad (27)$$

where  $s_N$  is the distance to the moving boundary at time  $t = (N - 1)\Delta t$

and  $\Delta t$  is the time increment in seconds.

The assumption that the local velocity at the boundary is equal to the rate of advance is valid for flow on an impermeable

bed. However, with infiltration the mean velocity a short distance behind the wetting front should be higher than the rate of advance since water must be flowing through the moving boundary to supply infiltration at the wetting front. Referring to Figure 7, if the water surface and infiltrated depth profiles are moving at some velocity  $w$  and are considered to be rigid for incremental time periods, then the local velocity at the moving boundary is given by

$$v_T = w \left( 1 + \frac{z_T}{Y_T} \right) , \quad - - - (28)$$

where  $z_T$  is the infiltrated depth at the moving boundary.

With a logarithmic infiltration function the intake rate at the wetting front is undefined. An initial intake rate at the moving boundary is defined by assuming a small constant intake opportunity time  $t_0$  at this point. This assumption also specifies  $z_T$ .

The determination of the advance rate has yet to be discussed. Methods which advance the wetting front by means of local flow conditions have been unsuccessful mainly because of the lack of suitable boundary conditions to maintain stability. A boundary condition on the system states that the total volume of water applied to a given time must be equal to the volume stored on the surface plus the infiltrated volume. The advance rate may be controlled in such a manner as to satisfy this condition at all times. The surface storage and infiltrated volumes must be calculated accurately for this method to be successful. The infiltrated volume is calculated at any time by integrating the infiltrated depth over all previous advance

increments as will be explained. The surface storage volume is integrated by a method such as Simpson's rule applied to the calculated depths at regular grid points.

Near the advancing front a finer grid spacing is needed than is required for the upstream portion of the profile. Immediately behind the moving boundary a front profile is formed on a moving grid parallel to the moving boundary. Figure 8 illustrates the method of calculating points for the front profile, which is a second degree polynomial fitted through three equally spaced points including the tip. The point spacing  $X$  is chosen sufficiently large so that the innermost point, say  $H_1$ , will lie on a backward characteristic from a point  $M$  on the previous front profile, while the intermediate point lies on a characteristic extended from the moving boundary. The directions of the backward characteristics are defined by Equation 25.

The depth and velocity at the tip or moving boundary are constant for each time increment. As a first approximation the front is advanced at the previously determined rate and the entire profile is calculated. The volumes are calculated and the error in the volume balance determined. If this error exceeds the allowable error the advance rate is readjusted and the intermediate point on the front profile recalculated. An iteration procedure is used to adjust the advance rate until the volume error is reduced to the desired level. When the solution is complete the velocities and depths at the front profile grid points are used to calculate interpolating polynomial coefficients for use in the next time increment.

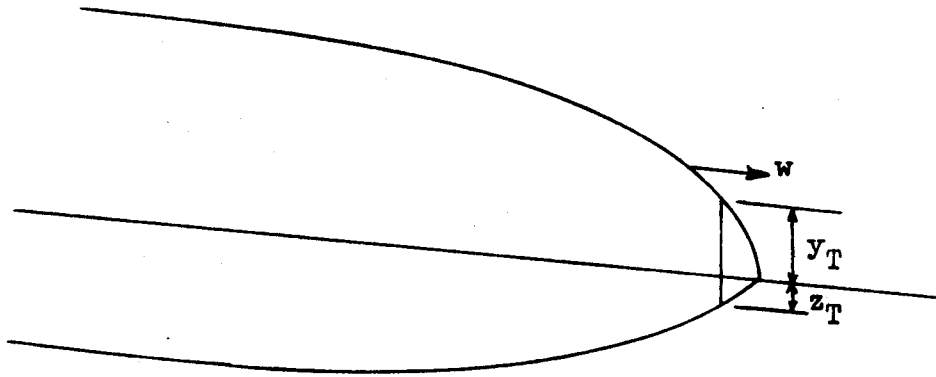


Figure 7. Advancing Profiles at the Wetting Front

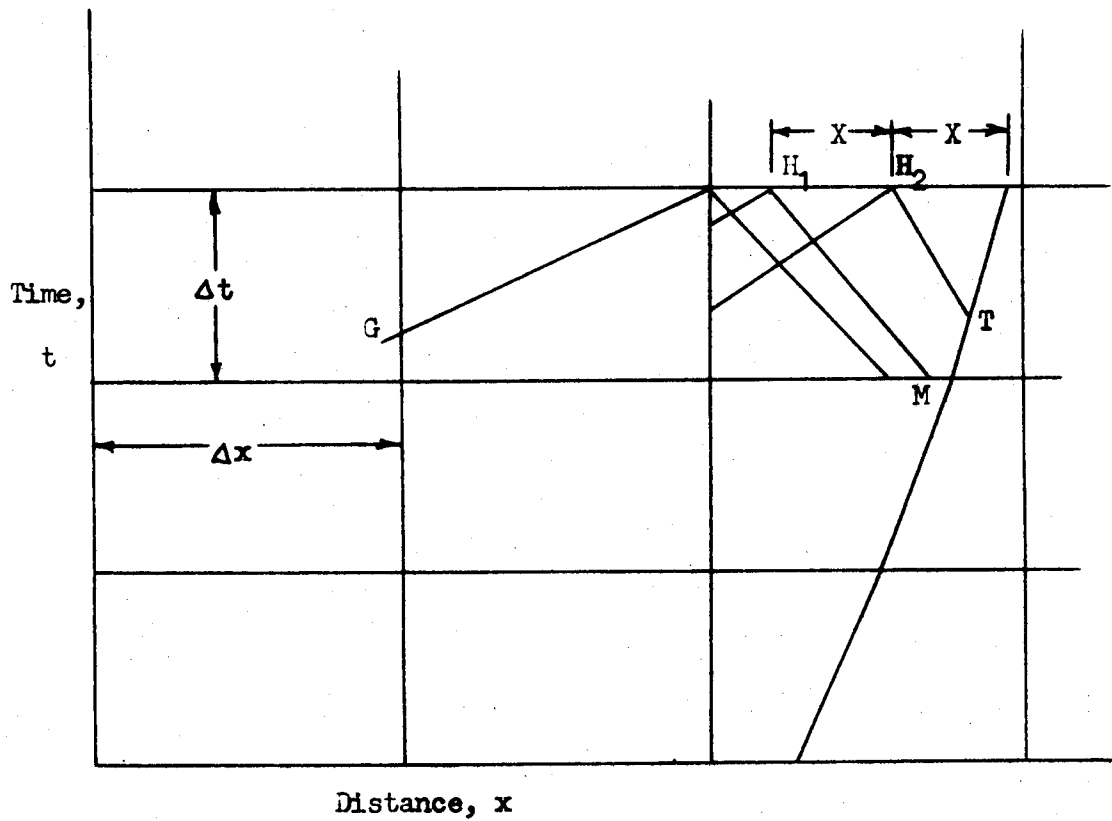


Figure 8. Calculating Points near the Moving Boundary

### Initiating a Solution

Figure 9 illustrates a method of determining the initial rate of advance and upstream depth. The boundary is extended for the first time increment at an assumed rate. The upstream boundary depth is then calculated by extending a backward characteristic to the moving boundary. The surface volume is calculated by assuming a parabolic water surface. After the first time increment, intermediate points may be calculated and the second degree curve fitted to form the front profile. When the moving boundary is beyond the first grid point, the moving grid has reached its maximum length and remains essentially constant.

An example solution is illustrated in Figure 10 after the solution has reached its final form. The average slope method is used to calculate the first 4 or 5 points behind the front profile. The grid spacing is then doubled and the remainder of the profile is calculated with the initial slope method. This enables the solution to be extended over long distances without increasing the computation time markedly for each time increment. With the time increment specified, the minimum grid spacing is determined by normal flow conditions in the relationship

$$\Delta x \geq (V_N + \sqrt{gY_N}) \frac{\Delta t}{2} \quad . - - - (29)$$

### Calculating the Infiltrated Volume

The moving boundary is advanced linearly over constant intervals of time. The advance distance is known for all time increments from the beginning of inflow. The infiltrated volume is determined by integrating Equation 2 with respect to x over each advance increment and summing all of these incremental

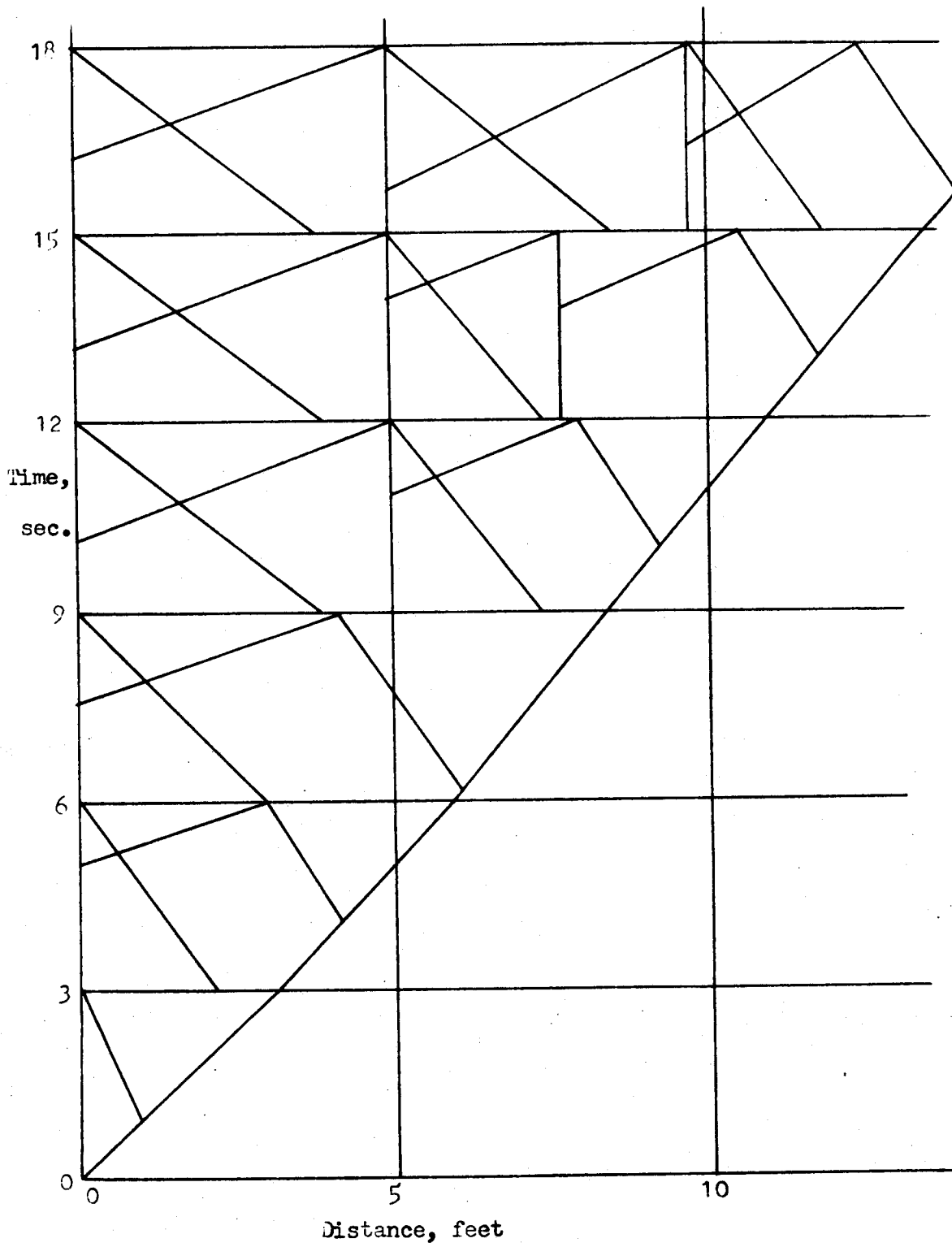


Figure 9. Initiating a Solution

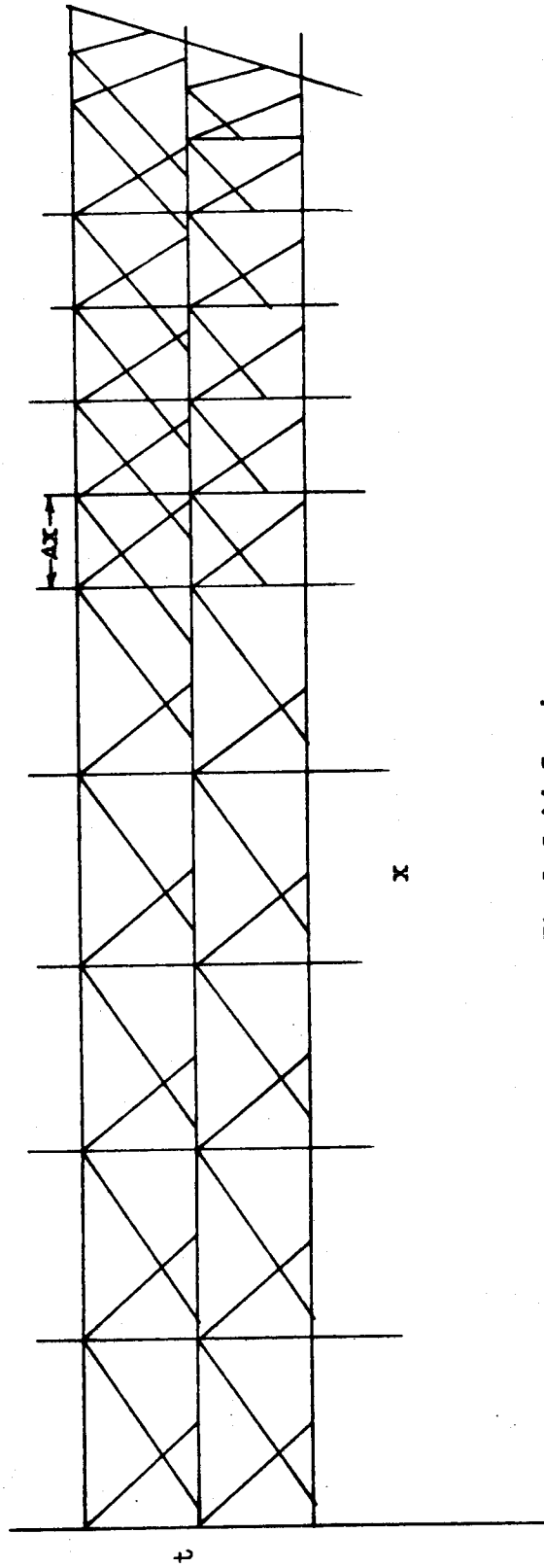


Figure 10. Final Grid Spacing

volumes. The result is the following relationship:

$$V_z = \frac{K}{\Delta t^{(a+1)}} \sum_{i=2}^N (s_i - s_{i-1}) \left[ (t_0 + (N-i+1)\Delta t)^{a+1} - (t_0 + (N-i)\Delta t)^{a+1} \right] \quad , \quad - \quad - \quad - \quad (30)$$

where  $V_z$  is the infiltrated volume per unit width at  $t = (N-1)\Delta t$

$\Delta t$  is the time increment

$t_0$  is the intake opportunity time defining the initial intake rate

$s_i$  is the advance distance at  $t = (i-1)\Delta t$ , ( $s_1=0$ )

and  $K$  and  $a$  are the infiltrated depth constants.

The units of  $K$  and  $a$  must, of course, be consistent with the time and distance units in Equation 30.

Evaluation of Results from the Hydrodynamic Model

In evaluating the effectiveness of the mathematical model in simulating border flow under field conditions, comparisons are made with experimental advance data, surface hydrograph data, and surface storage and infiltrated volume data. Five experimental borders were selected to obtain a wide range in slopes. Table 3 lists physical dimensions and slopes of the selected borders. Slopes for the first 500 feet are listed for borders 1M and 6M.

TABLE 3  
EXPERIMENTAL BORDERS

Border	Slope ft/ft	Length ft	Width ft
1M	0.00017	650	25.9
	.00020	500	
2M	.00038	770	25.6
3M	.00064	810	25.3
6M	.00075	850	25.1
	.00097	500	
5S	.00496	1112	30.2

Several irrigations were selected from the field data on the above borders. The calculated parameters for these irrigations are listed in Table 4. The infiltration constants were determined by the border infiltrometer method and by cylinder infiltrometers in some cases. These values for K and a give infiltrated depth in inches as a function of intake opportunity time in minutes, when used in Equation 2. The resistance parameters were calculated by the hydrograph analysis described previously. The listed values for Manning's n are the average of all values calculated from the data prior to shut off.

TABLE 4

IRRIGATION DATA

No.	Border	Date	q cfs/ft	Duration minutes	Infiltration		Constants		Manning n
					Border K	a	Cylinder K	a	
1	1M	61866	0.054	30	0.454	0.242			0.07
2	1M	80166	.037	82	.618	.259			.10
3	2M	71366	.055	55	.787	.151	.320	.311	.136
4	2M	81866	.04	110	.542	.306			.191
5	3M	71266	.058	48	.318	.428	.423	.283	.132
6	6M	61766	.082	43	.322	.334			.08
7	6M	62767	.062	51	.730	.224	.47	.36	.182
8	5S	82465	.059	65	.858	.161			.22
9	5S	41266	.068	105	1.060	.280			.19

The Effects of Tip Depth, Time Increment and Initial Infiltration Rate

The solution of the advance phase is examined with respect to the assumed depth and infiltration rate at the tip and the time increment at which the calculations are carried out. The purpose is to determine how critical the selection of these variables is to the accuracy of the overall solution. With this objective, several solutions were calculated using time increments of 3 to 6 seconds, tip depths of 0.02 to 0.1 feet, and values of  $t_0$  from 2 to 5 seconds.

The infiltration time lag  $t_0$  was found to be the least critical of the three calculation parameters. In order to maintain the ratio of tip velocity to rate of advance at values less than 1.2, it is necessary to use small values of  $t_0$ . The 2 second time lag was selected as optimum for use with the logarithmic infiltration function when the tip velocity is controlled by Equation 28.

With  $t_0 = 2$  seconds, the next step was to vary the time increment and tip depth and compare results. The parameters used in the following example were  $S_0 = .00097$ ,  $q = .082$ ,  $n = .07$ ,  $K = .322$  and  $a = .334$ . Three runs were made using time increments of 3 and 5 seconds while holding the ratio  $\Delta x/\Delta t$  constant at 2. The tip depth was specified initially and allowed to decrease in direct proportion to the advance rate as the solution progressed. Starting values for the tip depth were .06 and .09 feet.

The advance curves are shown in Figure 11 along with experimental advance data from Irrigation 6. The water surface profiles are shown in Figure 12 at a particular instant when the water had

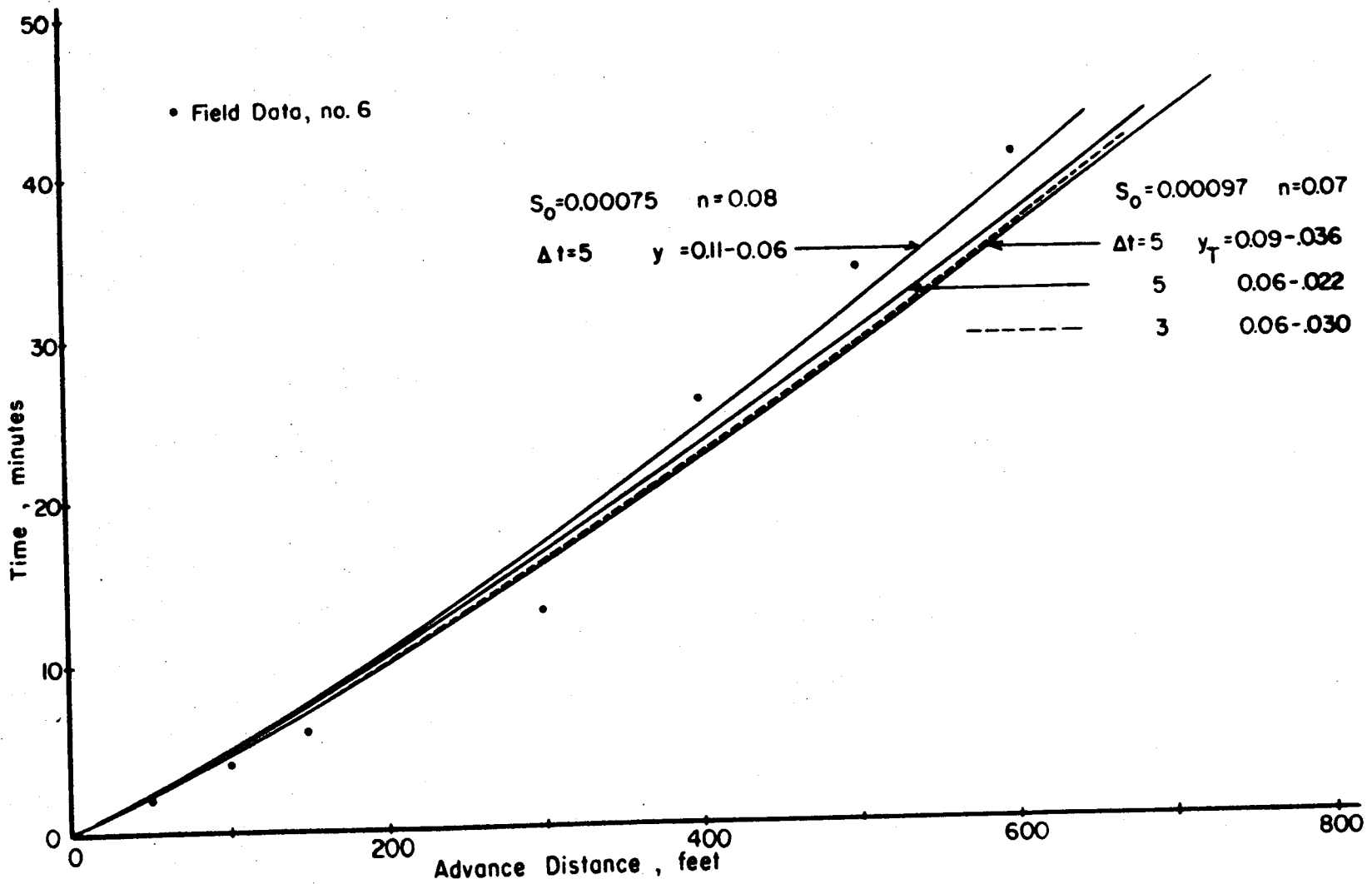


Figure 11. The Effect of Time Increment and Tip Depth on Advance

advanced about halfway down the border. The variation in the advance curve due to the above changes in the tip depth and time increment was less than 3 percent. Referring to Figure 12, it is apparent that the solution with the small tip depths and larger time increment did not give good results. If the tip depth is too small for a given time increment the trapezoidal integration from the moving boundary becomes inaccurate, causing a distortion in the profile in this region.

Figure 13 shows the experimental hydrographs from Irrigation 6. The theoretical hydrographs were recalculated up to 42 minutes using the parameters of irrigation 6 and a slope of 0.00075. The calculated hydrographs are superimposed in Figure 13 and the advance curve is plotted in Figure 11.

The surface storage and infiltrated volume curves as calculated from the field data for Irrigation 6 are compared in Figure 14 with the volume curves calculated in the numerical solution.

The wetting front, or the point of zero depth at any instant must be located ahead of the moving boundary. As the tip depth is decreased, the moving boundary should be shifted ahead and closer to the wetting front. However, it is apparent from the preceding figures that the boundary is shifted backward with smaller tip depths. This is a result of increased errors in the numerical approximations which cause the profile to become too steep at the tip. The velocities immediately behind the front may become unreasonably low under these conditions.

Thus, it is necessary to maintain a suitable balance between the tip depths and the time increment in order to obtain

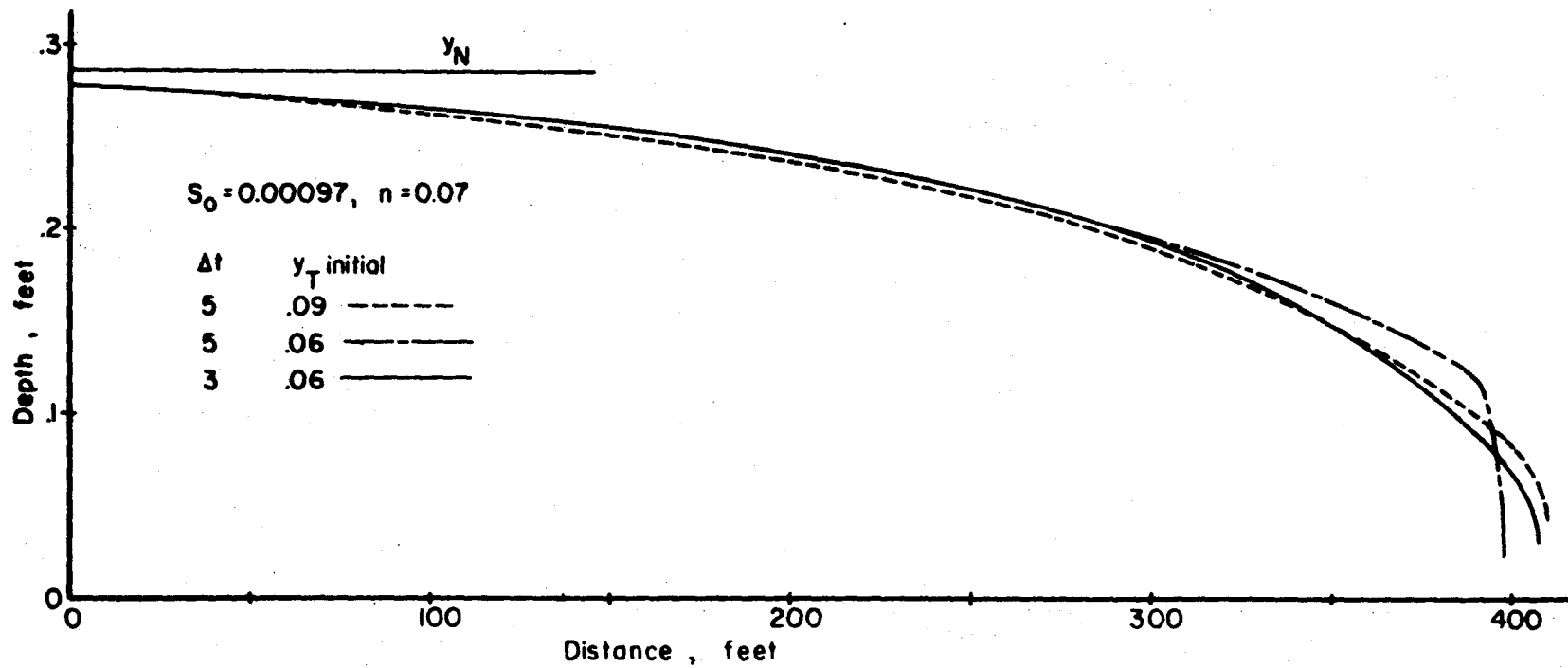


Figure 12. The Effect of Time Increment and Tip Depth on Water Surface Profiles

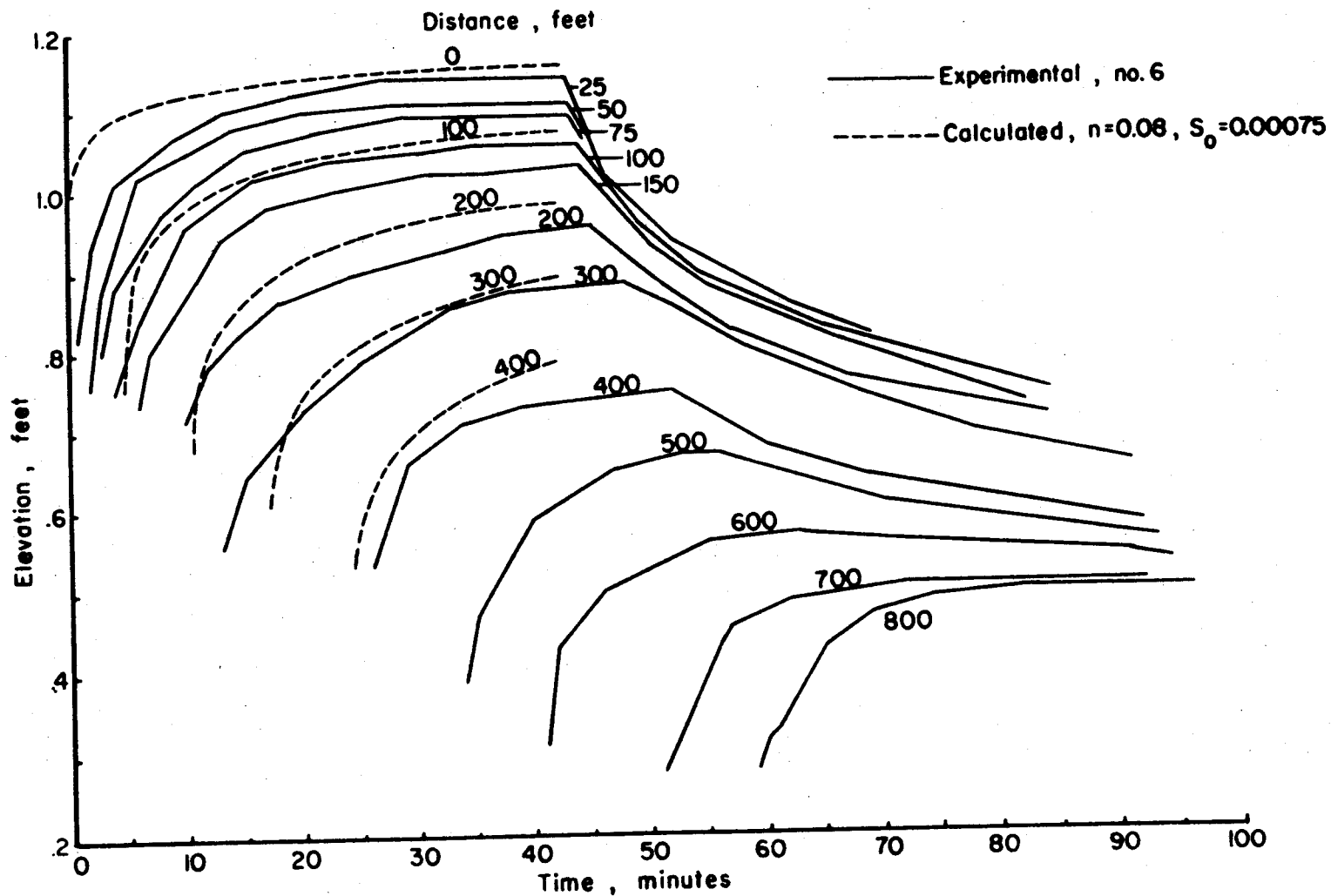


Figure 13. Experimental and Calculated Hydrographs for Irrigation 6

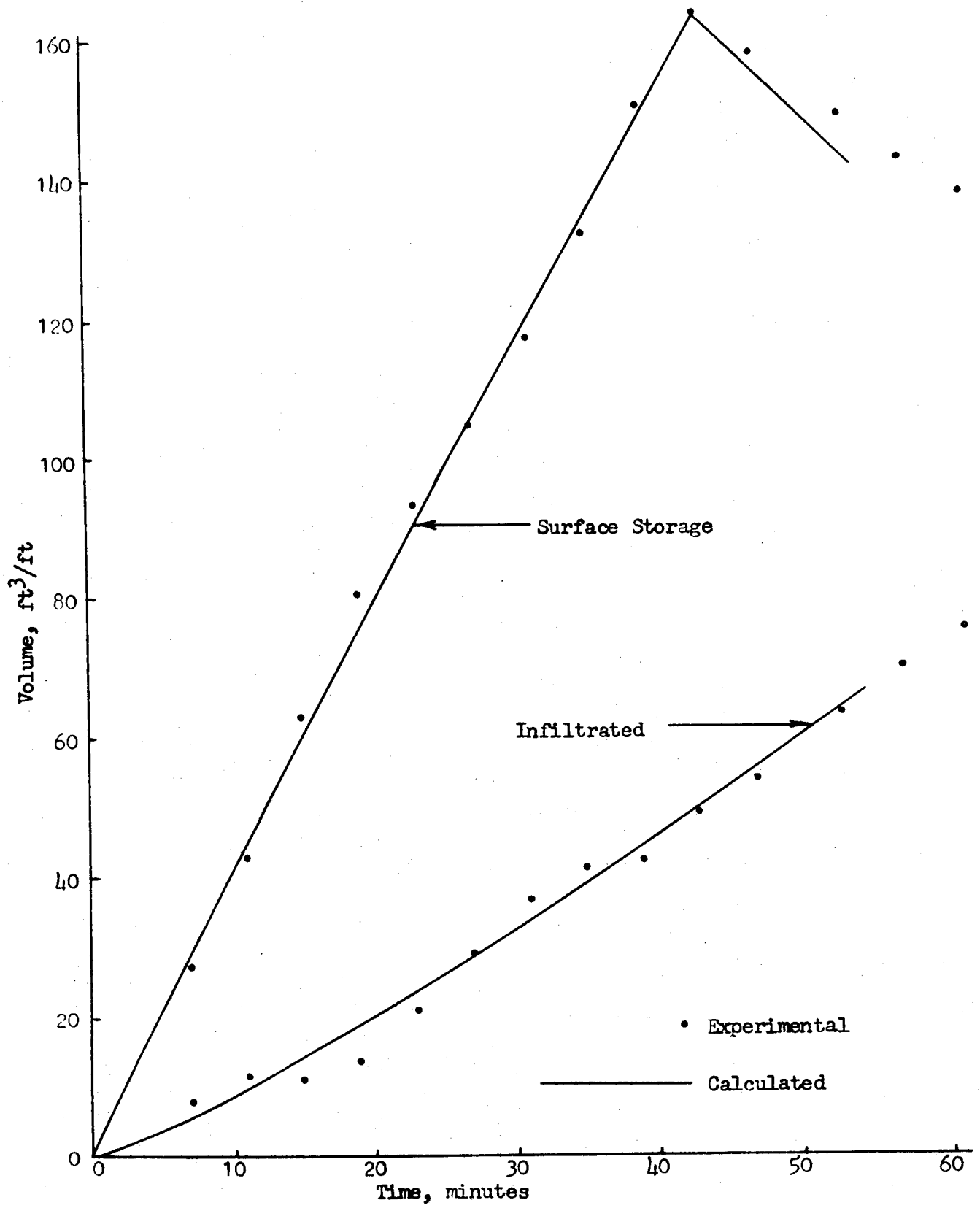


Figure 14. Surface Storage and Infiltrated Volumes

smooth velocity and depth profiles. With time increments of 3 to 5 seconds the tip depths should be maintained at 10 to 15 percent of normal depth. The front can be advanced over long distances with a constant tip depth after the first few minutes.

#### Non-Dimensional Surface Storage Relationships

The hydrodynamic model as described in the foregoing sections can be used to predict advance for any specified inflow conditions whenever the slope, infiltration and resistance characteristics of the border are known. The calculations are expensive in terms of computer time, particularly when small time increments are used. It is possible, however, to obtain general relationships which can be used in place of the numerical solutions with certain restrictions. The following analysis is limited to the condition of constant inflow rates.

Several simple volume balance techniques such as that of Hall (4) have been proposed for calculating advance. These methods require an estimate of the average surface depth at all times, and the accuracy of the result is limited by this estimate. The theoretical model is herein used to develop dimensionless surface storage-advance relationships for use in a volume-balance advance prediction.

A group of numerical solutions was calculated with a time increment of 3 seconds and a grid spacing  $\Delta x$  of 6 feet. The tip depth was initially specified as 25 percent of normal depth and allowed to decrease with the advance rate to 15 percent of normal depth where it was held for the remainder of the solution.

The local velocity at the tip was assumed to be equal to the advance rate and the time lag was set equal to 5 seconds.

The infiltration rates have a slight effect on the shape of the water surface and should not be neglected. However, in order to be able to generalize the results, it was necessary to use a fixed infiltration function. It was assumed that an average function would suffice to represent the infiltration rates in the numerical solutions. The constants chosen are  $K = 0.5$  and  $a = .3$ .

With the calculation parameters and the infiltration constants specified, a group of solutions was calculated on five different slopes using the combinations of discharge and resistance shown in Table 5. The normal depth and velocity for each solution are also listed.

TABLE 5

SELECTED PARAMETERS FOR THE NUMERICAL SOLUTIONS

Solution	$S_o$	n	q cfs/ft	$Y_N$ ft	$V_N$ ft/sec
1	0.0002	0.05	0.1	0.422	0.237
2	.0002	.1	.05	.422	.118
3	.0005	.1	.08	.425	.188
4	.001	.1	.08	.345	.231
5	.002	.1	.1	.321	.311
6	.002	.15	.08	.358	.223
7	.005	.15	.1	.311	.321

On a border of constant slope with a constant inflow rate, the upstream boundary depth gradually approaches normal depth while the average flow depth continually increases and approaches normal depth at a slower rate. Average depths are determined from the surface storage volumes calculated at each time increment in the numerical solutions. The water surface profiles are made dimensionless by dividing the depth and advance distance by the normal depth.

The ratio of the upstream boundary depth to the normal depth is plotted in Figure 15 for the solutions with parameters listed in Table 5. The upstream depth curve is essentially constant for a given slope. On the shallower slopes these curves are affected slightly by the resistance as seen by comparing solutions 1 and 2. The curves for solutions 5 and 6 essentially coincide, indicating less variation on the steeper slopes. Solution 3 was recalculated with  $K = 0$ , or zero infiltration. The dotted line in Figure 15 illustrates the effect of infiltration.

The ratio of the average depth to the upstream boundary depth is called the shape factor and is denoted by  $\sigma_y$ . The shape factor is plotted as a function of the dimensionless advance distance in Figure 16. These curves are less stable than the upstream depth curves since the shape of the water surface is affected by the infiltration rates and resistance. In general, the shape factor is increased slightly by a decrease in resistance or infiltration.

For purposes of predicting advance, it is convenient to represent the shape factor in a set of equations involving the dimensionless distance, the border slope and other factors if needed. Considering only the solid lines in Figure 16 which are for the

higher resistance, at  $s/y_N = 500$  the shape factor increases linearly with the border slope. The nonlinear portion of the curves is ignored since this region involves only the first 100 feet of advance in most cases. The shape factor is assumed constant for a given slope when the advance distance is less than 500 normal depths. Assuming the linear portion of the curves have a constant average slope,  $\sigma_y$  can be represented by the following equations.

$$\sigma_y = 0.7 + 30 S_o \quad s/y_N \leq 500$$

$$\sigma_y = 0.7 + 30 S_o + .00005(s/y_N - 500), \quad s/y_N > 500$$

The variation in shape factor due to infiltration and resistance is ignored because insufficient data has been generated to determine a more detailed relationship. The accuracy of these relationships is consistent with the accuracy and reliability of the numerical solutions themselves. They will yield good results for Manning's  $n$  in the range 0.05 to 0.2 and  $K$  values of 0 to 1.0.

The calculation of advance utilizing the dimensionless curves is accomplished by the same trial and error procedure used to advance the numerical solutions. The only difference is that the surface storage volume is determined by the average depth for a particular advance distance rather than by calculating the entire water surface profile. The moving boundary is advanced linearly over constant time intervals and the advance rate adjusted so that the volume balance is satisfied.

The surface storage volume is given by

$$V_y = y_N (y_U/y_N) \sigma_y s$$

for any given value of  $s$ . The interpolation between the upstream depth curves should be semi-logarithmic, i.e. values of  $y_U/y_N$  are interpolated linearly between values of  $10g S_o$  at constant distances.

Several advance curves have been calculated using the dimensionless curves and the irrigation data from Table 4. These curves are shown in Figures 17-19 for comparison with the experimental advance data. The advance was calculated with cylinder infiltrometer constants for Irrigations 3, 5, and 7.

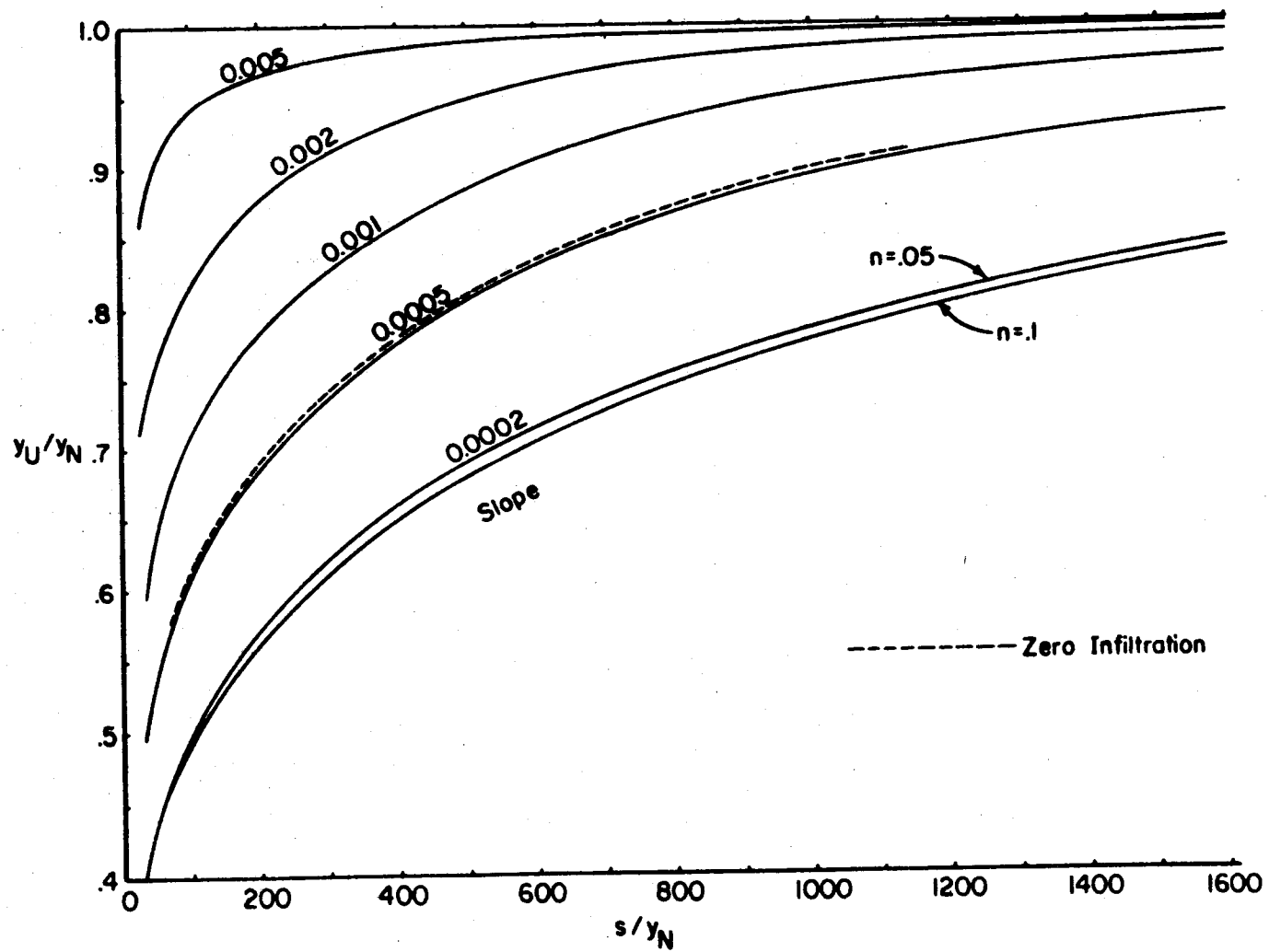


Figure 15. Dimensionless Upstream Depth versus Dimensionless Advance Distance

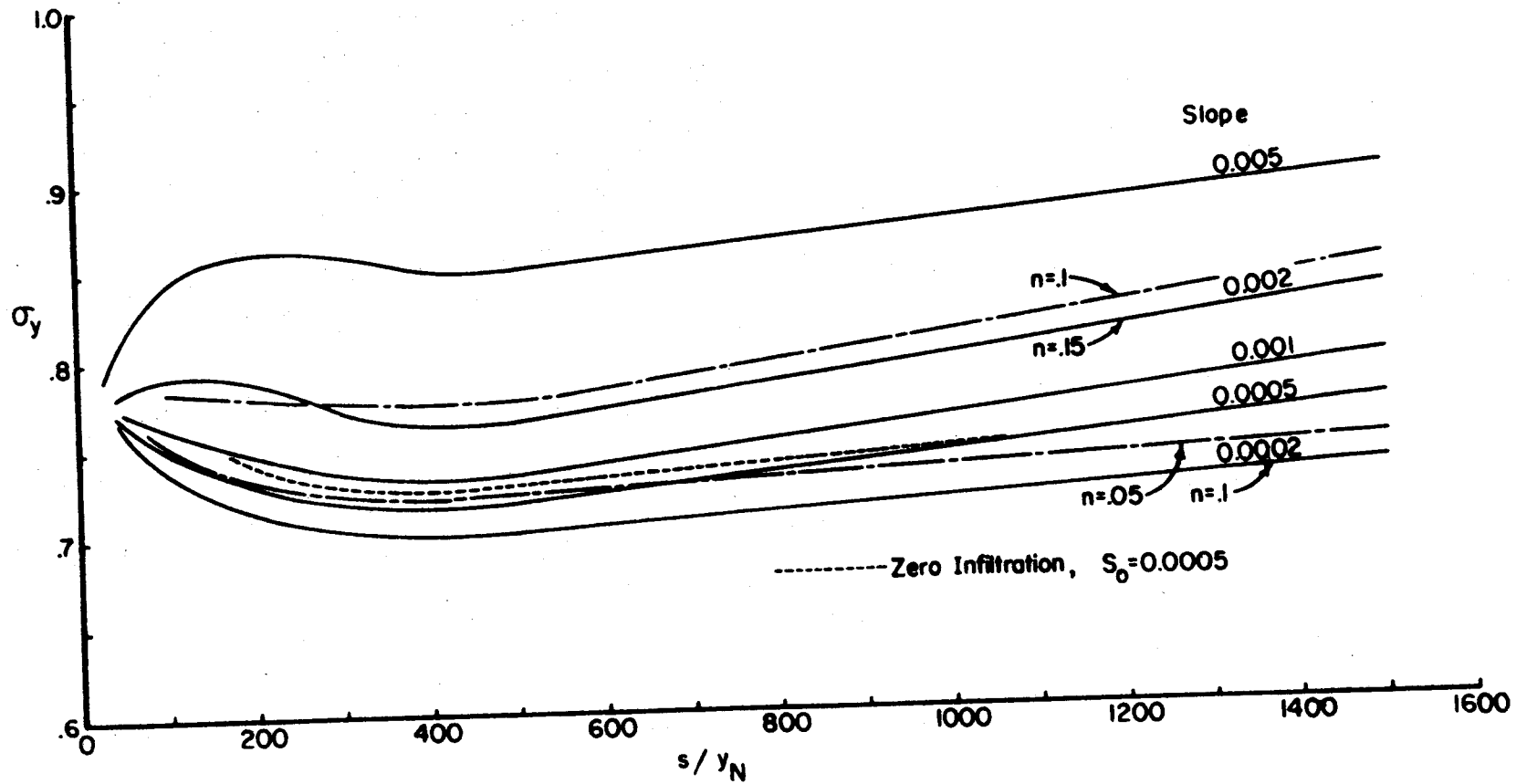


Figure 16. Dimensionless Average Depth versus Dimensionless Advance Distance

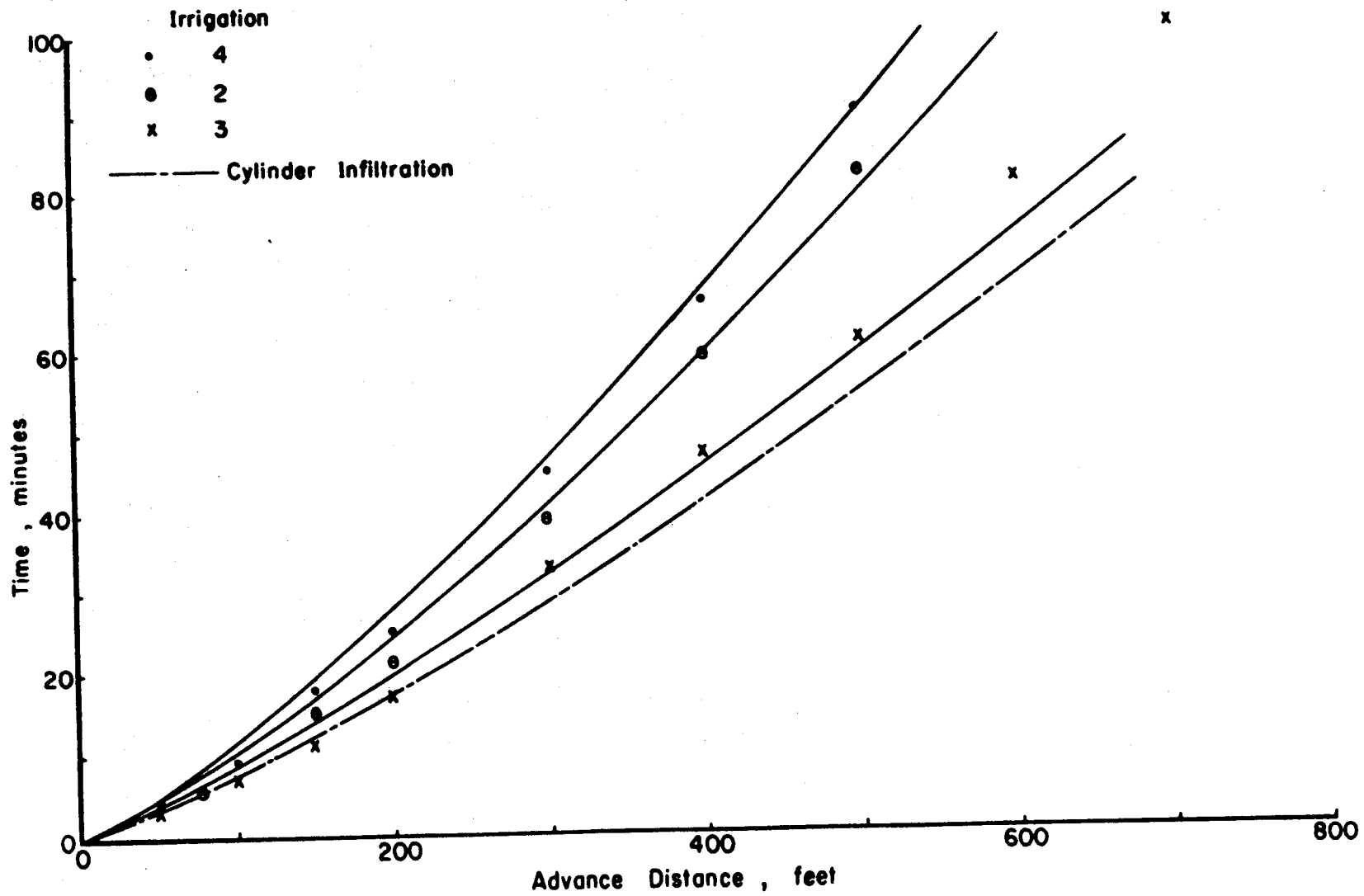


Figure 17. Advance Curves for Irrigations 2, 3 and 4

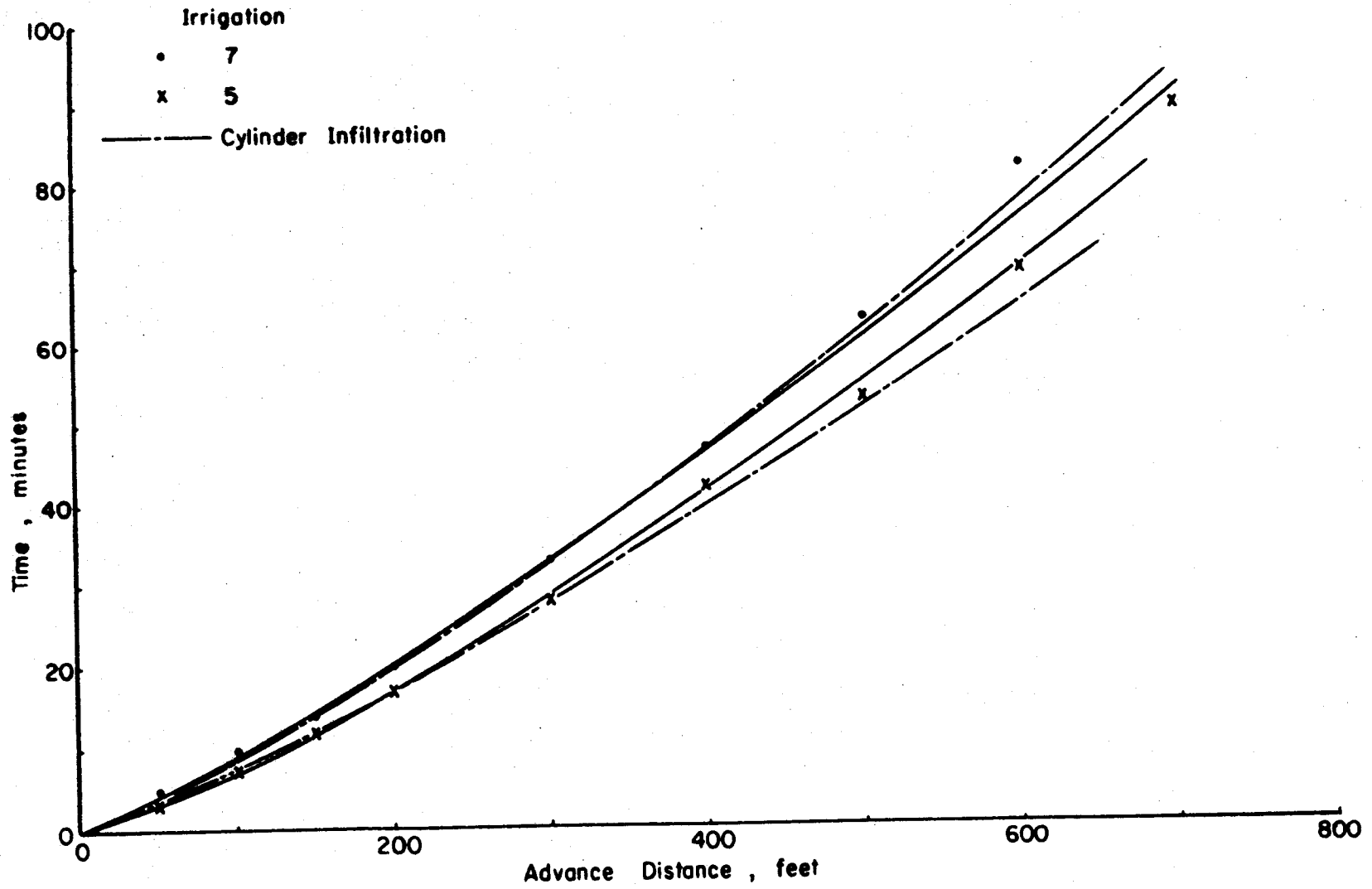


Figure 18. Advance Curves for Irrigations 5 and 7

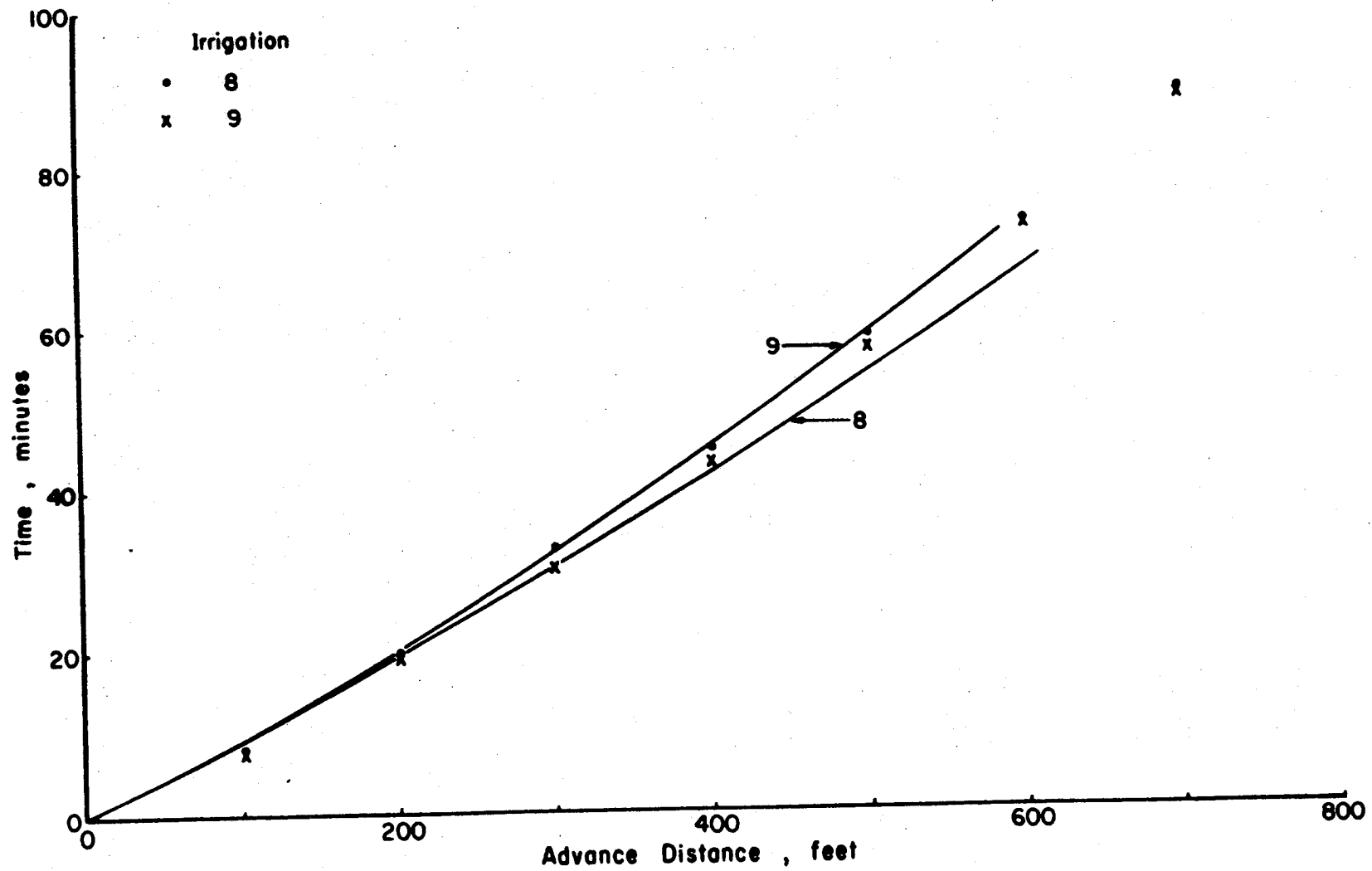


Figure 19. Advance Curves for Irrigations 8 and 9

#### IV. Summary

The study of surface irrigation hydraulics in Colorado began in 1955 with the objective of developing a rational irrigation system design procedure. Methods of characterizing the infiltration and hydraulic resistance of the soil were needed. The initial studies determined that the soil roughness can be characterized by the standard deviation of equally spaced roughness height measurements and that hydraulic resistance can be predicted by this parameter alone.

Recent studies have focused attention on the infiltration characteristics of irrigated soils. Experiments designed to study infiltration and hydraulic resistance also yielded information concerning operating criteria for maximum irrigation efficiency in border systems.

The objectives of the final phase of the study which this report covers were: (1) to determine infiltration parameters by cylinder infiltrometers and compare with the parameters using the entire border as an infiltrometer, (2) to calculate resistance parameters from surface flow data, and (3) to utilize the calculated parameters in a rational design procedure.

The infiltration analysis yielded constants for a logarithmic intake function from both the borders and cylinder infiltrometers. The two methods are compared by calculating infiltrated depths at a given time with the infiltration constants determined by the border method and by the cylinder method. The results show that on a clay loam soil prone to cracking, the border

infiltration constants predict infiltrated depths nearly twice as high as those determined by the cylinder constants.

The effect of the infiltration function in predicting advance of an irrigation stream is shown by differences in calculated advance distances when using the border and cylinder infiltrometer constants.

A volume balance method is used to calculate flow rates and hydraulic resistance after the infiltration constants have been determined. Energy gradients are determined by fitting a straight line through total head data. With the average depth, velocity and energy gradient known, parameters can be calculated for any resistance function.

For optimum design, a rational method of predicting advance and recession rates is needed. The hydrodynamic equations of unsteady flow provide a means of simulating border irrigation for any specified inflow conditions when the slope, infiltration and resistance characteristics of the border are known.

A numerical solution of the momentum and continuity equations is accomplished by the method of characteristics. The solutions are advanced on a rectangular grid network in the time-distance plane by solving the finite difference equations for the depth and velocity at successive grid points.

The downstream boundary is specified as the locus of points at a small assumed depth. The rate of advance of the moving boundary is controlled by the overall continuity of the system. That is, the sum of the surface storage and infiltrated volumes at any instant is kept equal to the total volume applied. Assumptions concerning the depth and infiltration rate at the moving boundary are examined, as well as the time increment at which the solutions

are carried out.

The logarithmic infiltration function is used to determine infiltration rates and infiltrated volumes in the mathematical model. A resistance function of the form of the Manning or Chezy equation is used to define the energy gradient.

Numerical solutions calculated on a wide range of slopes with constant inflow rates are generalized by dividing the depth and advance distance by the normal flow depth. This results in dimensionless relationships which give the average surface storage depth as a function of the advance distance. With these relationships known, a simple volume balance technique may be used to predict advance with constant inflow.

Work which remains to be done includes extension of the hydrodynamic theory to the recession phase. The model will then simulate the entire irrigation and can be used to predict advance and recession for variable inflow rates. Finally, the results obtainable with this theory will be integrated into a design procedure.

## LITERATURE CITED

1. Gilley, James R., Intake function and border irrigation. Unpublished Masters Thesis, Colorado State University, Fort Collins, Colorado, June 1968.
2. Haise, Howard R., W. W. Donnan, J. T. Phelan, L. F. Lawhon and D. G. Shockley, The use of cylinder infiltrometers to determine the intake characteristics of irrigated soils. ARS and SCS, ARS 41-7.
3. Haise, Howard R., Automation of irrigation: need and potential. Proceedings SCSA 24th Annual Meeting, p. 74-76, 1969.
4. Hall, Warren A., Estimating irrigation border flow. Agricultural Engineering, 37:(4) 263-265, April 1956.
5. Heermann, Dale, F., Hydraulics of small open channels. Unpublished Masters Thesis, Colorado State University, Fort Collins, Colorado, 1964, 74 p.
6. Heermann, Dale F., Characterization of hydraulic roughness. Unpublished Ph.D. Dissertation, Colorado State University, Fort Collins, Colorado, August, 1968.
7. Howe, O. W. and D. F. Heermann, Efficient border irrigation design and operation. American Society of Agricultural Engineers, Transactions 13:(1) 126-130, 1970.
8. Kincaid, Dennis C., Hydrodynamics of border irrigation. Unpublished Ph.D. Dissertation, Colorado State University, Fort Collins, Colorado, August 1970.
9. Koloseus, H. J. and J. Davidian, Free-surface instability correlations and roughness-concentration effects on flow over hydrodynamically rough surfaces. Geological Survey Water Supply Paper 1592c-d, 1966, 93 p.
10. Kostiaikov, A. N., On the dynamics of the coefficient of coefficient of water percolation in soils and on the necessity for studying it from a dynamic point of view for purposes of amelioration. Trans. 6th Com. Intern. Soc. Soil Sci. Russian Part A: 17-21.
11. Kruse, E. G., C. W. Huntley and A. R. Robinson, Flow resistance in simulated irrigation borders and furrows. Conservation Research Report No. 3, ARS, USDA, November 1956, 56 p.

12. Lewis, M. R. and W. E. Milne, Analysis of border irrigation. Agricultural Engineering, 19: 267-272, June 1938.
13. Philip, J. R. and D. A. Farrell, General solution of the infiltration advance problem in irrigation hydraulics. Journal of Geophysical Research, 69: 621-631, February 1964.
14. Sayre, W. W. and M. L. Albertson, Roughness spacing in rigid open channels. American Society of Civil Engineers, Proceedings, Vol. 87, HY3, p. 121-150, May 1961.
15. Schlichting, Hermann, Experimentelle untersuchungen zum rauhgheitsproblem. Ingenieur-Archiv., Vol. 7, No. 1, 1936, p. 1-34. (Translation NACA Technical Memo 823, April 1937)
16. Shockley, Deil G., H. J. Woodward and John T. Phelan, A quasi-rational method of border irrigation design. Presented at the Winter Meeting of the American Society of Agricultural Engineers, Chicago, Illinois, 1963.
17. Wenstrom, Richard J., Flow resistance in irrigation furrows. Unpublished Masters Thesis, Colorado State University, Fort Collins, Colorado, 1966, 100 p.
18. Willardson, Lyman S. and A. Alvin Bishop. Analysis of surface irrigation application efficiency. Proceedings of the American Society of Civil Engineers, Journal of the Irrigation and Drainage Division, IR2, June 1967.